

Chapter 3

Potential Energy

The macroscopic interaction energy between two heavy ions is usually given as a sum of a Coulomb-energy and a nuclear term. The problem of determining the nuclear part of the interaction is one of the important and as yet not completely solved problems of low-energy nuclear physics.

One of the most common ways to obtain information about the interaction of two nuclei is to analyze the experimental data on the elastic scattering of heavy ions. This is done in the framework of the optical model, the overwhelming majority of studies being based on the Woods-Saxon form of the nuclear potential, which was originally used to describe elastic neutron-nucleus scattering. There are well-known difficulties with the optical model associated with ambiguity in the determination of the parameters of the potential due to incompleteness of the experimental data sets. Moreover the result the analysis of the experimental data is to large extent influenced by the particular assumption made on the radial dependence of the potential. By adjusting the parameters of the Woods-Saxon potential using specific experimental data, a correct description of the behavior of the potential in a narrow range of distances R is achieved. For a physically justified parametrization the behavior of the potential outside the region of sensitivity must be stable with respect to small changes in the masses of colliding nuclei. In contrast, an inappropriate parametrization may result in a phenomenological potential which becomes physically meaningless outside the region of sensitivity.

Therefore it is natural to seek for an alternative to the Woods-Saxon potential, like for example the theoretical calculation of a ion-ion potential, which despite its approximate nature, can correctly reflect the qualitative dependence of the interaction masses, the collision energy, and the distance between nuclei.

Due to the complexity of the many-particle problem in the heavy-ion collisions or decays, it is customary analyzed within two extreme approximations - the adiabatic and the sudden(diabatic) models.

In the first approximation the approach(distancing) of the centers of mass of the colliding(decaying) ions is accompanied by a smooth adiabatic change in the internal structure of the ions, the equilibration of the nuclear densities being energetically favored for each distance. When an adiabatic collision(decay) occurs, it is necessary that the relaxation rate of the internal degrees of freedom of the target(larger cluster) be large compared with the translational velocity of the projectile(lighter cluster) In adiabatic models the liquid-drop model

lead to a correct connection between the properties of normal nuclear matter and the behavior of the potential at the edge of the nucleus but its applicability fails in the interior region of the potential, i.e. in the strong overlapping region of the colliding or decaying nuclei.

In the second approximation, the collision(decay) occurs so rapidly that the internal structure of the ions cannot change significantly during the interaction time. In this case, the nucleon densities of the nuclei in the region of their overlap are simply added, and this, unavoidably leads to the occurrence of a strong short-range repulsive core in the potential. In other words, models based on the sudden approximation with allowance for the Pauli principle predict the existence in the interaction potential of a strong repulsion when the ion densities are sensitively overlapping, thus preventing the nuclei from penetrating each other. This property is specific for composite systems of fermions and is not related to the repulsive core in the nucleon-nucleon potential. The existence of a short-range repulsion follows from existing microscopic calculations of ion-ion interaction based on the approximate solution of the many-particle Schrödinger equation with a two-body nucleon-nucleon potential.

A measure of the adiabaticity or diabaticity is given by the ratio k/k_F , where $k = \sqrt{(2m/\hbar^2)E/A}$ is the mean translational momentum of a nucleon in the projectile, and k_F is the Fermi momentum for the internal motion of nucleons inside the nucleus. If $k \gg k_F$, a sudden collision can be expected. In the opposite case, case i.e. $k \ll k_F$ an adiabatic collision occurs. Let us make a rough evaluation for the case of cold fission. For the Fermi momentum we take the infinite matter ansatz [1], i.e. $k_F = (3\pi^2\rho/2)^{1/3}$, which for a constant density reads $k_F = (9\pi)^{1/3}/2r_0$. For A we take the value 100 corresponding to a possible cluster emitted in the cold decay of ^{252}Cf and for E a value of 200 MeV comparable to the cold decay Q -value. The evaluation gives $k/k_F \approx 0.25$. For nuclei from the superheavy island ($Z=112-122$) synthesised with in cold reactions we obtain values within the same order of magnitude. This means that cold fission and fusion reactions of heavy and are superheavy nuclei are apparently inbetween the two extremes. For this reason both model will be applied throughout this work and especially the sudden model.

3.1 Liquid-Drop Model

The most simple example of adiabatic model in calculating the interaction potential between two heavy ions is the method based on a representation of the nucleus as a liquid drop of incompressible nuclear matter. The Liquid drop Model (LDM) was originally conceived in the mid-thirties of the last century by C.F. von Weizsäcker with the task to calculate ground state nuclear binding energies [2]. It was recognized at that time that gross properties of nuclear fission could be understood in terms of the shape dependence of the surface and electrostatic energies. One of the most simple Ansatz of the LDM mass formula is the sum of the individual proton M_Z and neutron M_N masses reduced by the binding energy [3].

$$M_{LD}(N, Z) = M_N N + M_Z Z - c_V A + c_S A^{2/3} B_{\text{surf}} + \frac{3}{5} \frac{e^2 Z^2}{r_0 A^{1/3}} \left(B_{\text{coul}} - \frac{5}{6} \pi^2 \frac{d^2}{r_0^2 A^{2/3}} - \frac{0.7636}{Z^{2/3}} \right) \quad (3.1)$$

In deriving eq.(3.1) it was assumed that the nuclear matter in the interior is uniform and incompressible so that the radius of the spherical nucleus is proportional to $A^{1/3}$. The assump-

tion of incompressibility means that in a collision of heavy ions one can admit all volume preserving deformations of their shapes.

The last three terms in the above formula are accounting for the binding energy . The first of these terms is called the *volume energy* and is proportional to the total number of particles.

3.1.1 The Geometrical Surface Energy

The next term in (3.1) is the *surface energy* , the factor $A^{2/3}$ being proportional to the surface area for a spherical nucleus. To deal with different types of surfaces the quantity B_{surf} is introduced. It relates the surface energy of a deformed nucleus, $E_{\text{surf}} = \sigma \int dS$ (σ -surface tension given in units of MeV/fm²) to that of a spherical nucleus, $E_s^0 = 4\pi R_0^2 \sigma$, with the same volume :

$$B_{\text{surf}} = \frac{E_{\text{surf}}}{E_s^0} = \frac{1}{4\pi R_0^2} \int dS \quad (3.2)$$

The integration is performed over the volume of the nuclear configuration, whose magnitude is held fixed at $4\pi R_0^3/3$ as the nucleus deforms. The equivalent-sharp-surface radius R_0 of the spherical nucleus is related to the nuclear-radius constant r_0 by

$$R_0 = r_0 A^{1/3} \quad (3.3)$$

In cylindrical coordinates (3.2) reads

$$B_{\text{surf}} = \frac{1}{2R_0^2} \int_{z_L}^{z_R} \rho(z) \sqrt{1 + \left(\frac{d\rho(z)}{dz}\right)^2} dz \quad (3.4)$$

where z_L and z_R are the left and right tips (poles) of an axial-symmetric nucleus. Using the parametrization of Myers and Swiatecki [3] we have that

$$E_s^0 = 17.9439 \left[1 - 1.7826 \left(\frac{A - 2Z}{A} \right)^2 \right] A^{2/3} \text{MeV} \quad (3.5)$$

Pashkevich [4] proposed another ansatz

$$E_s^0 = 21.13 \left[1 - 2.3 \left(\frac{A - 2Z}{A} \right)^2 \right] A^{2/3} \text{MeV} \quad (3.6)$$

3.1.2 Yukawa-Plus-Exponential Potential

Eq.(3.1) results from an expansion of the nuclear energy in powers of $A^{-1/3}$ and relative neutron-proton excess $I = [(N - Z)/A]^2$ (leptodermous expansion) [3]. This expansion is valid only if all geometrical dimensions of the drop are large compared to the surface thickness, and consequently breaks down for two nearly touching nuclei and for shapes with small necks, for example around the scission point in fission or first contact in heavy-ion reactions. The liquid-drop formula yields a spurious and undesirable sensitivity of the calculated fission barriers on unphysical fine details of the shape in the neck region. Therefore a generalization of the liquid-drop formula was proposed which satisfies the following conditions :

- It should reproduce the result of the old liquid-drop formula for spherical configurations.
- It should not be sensitive to the high multipole wiggles on the surface of the drop.
- There should be an attractive nuclear interaction energy between two separated fragments besides the Coulomb repulsion. The range of this attractive force should extend beyond the equivalent sharp radius by roughly the range of the nucleon-nucleon interaction. One should require the minimality of the surface energy of the two half-spaces of nuclear matter at the instant when they touch.

In the original single-Yukawa modified liquid drop model [5] the surface energy $E_{\text{surf}} = E_S^0 B_{\text{surf}}$ was replaced by

$$E_n = E_Y(a, c_S) + \frac{2r_0}{3} \frac{c_S A}{a} \quad (3.7)$$

where

$$E_Y(a, a_s) = -\frac{c_S}{8\pi^2 r_0^2 a^3} \int \int \frac{e^{-|\mathbf{r}-\mathbf{r}'|/a}}{|\mathbf{r}-\mathbf{r}'|} d^3r d^3r' \quad (3.8)$$

and the quantity a is the range of the Yukawa folding function. In the limit $a \rightarrow 0$, eq.(3.7) yields exactly the surface energy of the liquid-drop formula (3.1). The effective surface-energy constant c_S depends on the relative neutron-proton excess

$$c_S = a_S(1 - \kappa_S I^2) \quad (3.9)$$

where a_S is the surface energy constant and κ_S is the surface-asymmetry constant. The second term in (3.7) cancels the volume-energy term present in the double volume integral of the Yukawa function. However the single-Yukawa potential violates the requirement that for a saturating nuclear system the interaction energy per unit area reach a minimum at touching. This saturation condition can be satisfied by the use of the Yukawa-plus-exponential form of the interaction [6]

$$E_n = -\frac{c_S}{8\pi^2 r_0^2 a^3} \int \int \left(\frac{|\mathbf{r}-\mathbf{r}'|}{a} \right) \frac{e^{-|\mathbf{r}-\mathbf{r}'|/a}}{|\mathbf{r}-\mathbf{r}'|} d^3r d^3r' \quad (3.10)$$

The above integral would be zero if the integrations over \mathbf{r} and \mathbf{r}' were both extended over all space. Consequently this new form of the potential does not contain a volume term and does not require volume renormalization. A two-fold application of the Gauss divergence theorem transforms (3.10) into the double surface integral [7]

$$E_n = -\frac{c_S}{8\pi^2 r_0^2} \oint \oint \left\{ 2 - \left[\left(\frac{|\mathbf{r}-\mathbf{r}'|}{a} \right)^2 + 2 \frac{|\mathbf{r}-\mathbf{r}'|}{a} + 2 \right] e^{-\frac{|\mathbf{r}-\mathbf{r}'|}{a}} \right\} \\ \times \frac{(\mathbf{r}-\mathbf{r}') \cdot d\mathbf{S}(\mathbf{r}-\mathbf{r}') \cdot d\mathbf{S}'}{|\mathbf{r}-\mathbf{r}'|^4} \quad (3.11)$$

This is a four-fold integral which has to be computed numerically for arbitrary shapes. For an axially symmetric, but otherwise arbitrary shape, one of the azimuthal integrations can be

performed trivially. With the nuclear surface specified in cylindrical coordinates (ρ, ϕ, z) by the equation

$$\rho = \rho(z) \quad (3.12)$$

we obtain a threefold integral

$$\begin{aligned} E_n &= \frac{c_S}{4\pi^2 r_0^2} \int_{z_L}^{z_R} \int_{z_L}^{z_R} \int_0^{2\pi} \left\{ 2 - \left[\left(\frac{|\mathbf{r} - \mathbf{r}'|}{a} \right)^2 + 2 \frac{|\mathbf{r} - \mathbf{r}'|}{a} + 2 \right] e^{-\frac{|\mathbf{r} - \mathbf{r}'|}{a}} \right\} \\ &\times \rho(z) \left[\rho(z) - \rho(z') \cos \phi - \frac{d\rho(z')}{dz} (z - z') \right] \\ &\times \rho(z') \left[\rho(z') - \rho(z) \cos \phi - \frac{d\rho(z')}{dz} (z' - z) \right] \frac{dz dz' d\phi}{|\mathbf{r} - \mathbf{r}'|^4} \end{aligned} \quad (3.13)$$

where the integrations over z and z' extend from the left tip of the shape located at z_L to the right one located at z_R and the ϕ integration extends from 0 to 2π . For an axially symmetric shape the distance $|\mathbf{r} - \mathbf{r}'|$ is given by

$$|\mathbf{r} - \mathbf{r}'| = \sqrt{\rho^2(z) + \rho^2(z') - 2\rho^2(z)\rho^2(z') \cos \phi + z^2 + z'^2 - 2zz'} \quad (3.14)$$

The nuclear finite-range energy corresponding to a sphere reads

$$E_n^0 = E_S^0 \left\{ 1 - 3 \left(\frac{a}{r_0} \right)^2 + \left(1 + \frac{r_0}{a} \right) \left[2 + 3 \frac{a}{r_0} + 3 \left(\frac{a}{r_0} \right)^2 \right] e^{-\frac{2r_0}{a}} \right\} \quad (3.15)$$

Taking the free parameters to have the values $r_0 = 1.18$ fm, $a = 0.65$ fm, $a_S = 21.7$ MeV and $\kappa_S = 3.0$, Krappe, Nix and Sierk [6] were able to obtain a good description of a large collection of experimental data relating to the nuclear masses and deformations, the fusion and fission barriers, and the differential cross-sections of heavy-ion small angle elastic scattering .

To compare the surface reduced energy with the finite-range one we represented in fig.3.1, the upper panel, the two curves as a function of the elongation ε for two different α_3 . It is to be noticed that the difference the two curves increase with ε . The finite range energy has a smaller rate of increase. Beyond $\varepsilon=1$, when rupture occurs, the surface energy is saturating.

3.1.3 Coulomb Potential

The last term in eq.(3.1) is the *Coulomb energy* and contains the factor B_{Coul} which relates the actual Coulomb energy of a deformed nucleus,

$$E_{\text{Coul}} = \frac{1}{2} \int d\mathbf{r} \int d\mathbf{r}' \frac{\rho(\mathbf{r})\rho(\mathbf{r}')}{|\mathbf{r} - \mathbf{r}'|}, \quad (3.16)$$

to that of a spherical nucleus, $E_C^0 = \frac{3}{5} \frac{e^2 Z^2}{R_0}$, of the same volume

$$B_{\text{Coul}} = \frac{E_{\text{Coul}}}{E_C^0} \quad (3.17)$$

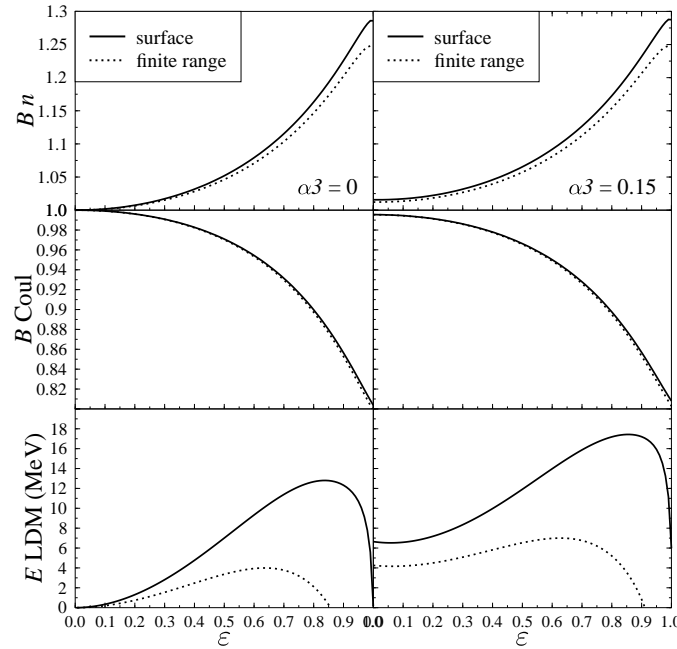


Figure 3.1: Surface and finite-range reduced energies (upper panel), Coulomb reduced energies with and without finite-range corrections (middle panel) and LDM deformation energies with and without finite-range corrections (lower panel) for reflexion-symmetric shapes ($\alpha_3 = 0$) and reflexion-asymmetric shapes ($\alpha_3 = 0.15$).

and in cylindrical coordinates

$$B_{\text{Coul}} = \frac{1}{2R_0^2} \int_{z_L}^{z_R} \Phi_s(z) \left(\rho(z)^2 - z\rho(z) \frac{d\rho(z)}{dz} \right) dz \quad (3.18)$$

where

$$\Phi_s(z) = \frac{3}{4\pi R_0^2} \int d\bar{z} \frac{k}{\sqrt{\rho(z)\bar{\rho}(\bar{z})}} \left\{ \left[\rho(z)\bar{\rho}(\bar{z}) + \bar{\rho}^2(\bar{z}) + (z - \bar{z})\rho(z) \frac{d\bar{\rho}(\bar{z})}{d\bar{z}} \right] K(k^2) - 2\rho\bar{\rho}D(k^2) \right\} \quad (3.19)$$

$K(k^2)$ and $D(k^2) = [K(k^2) - E(k^2)]/k^2$ being complete elliptic integrals of the argument

$$k^2 = \frac{4\rho(z)\bar{\rho}(\bar{z})}{(z - \bar{z})^2 + (\rho + \bar{\rho})^2}$$

(see [8], p.74, eq.(7.10)).

The Coulomb energy of a charged sphere is according to Myers and Swiatecki [3]

$$E_c^0 = 0.7053 \frac{Z^2}{A^{1/3}} \text{MeV} \quad (3.20)$$

and to Pashkevich [4]

$$E_c^0 = \frac{32}{(Z^2/A)_{cr}} \frac{Z^2}{A^{1/3}} \quad (3.21)$$

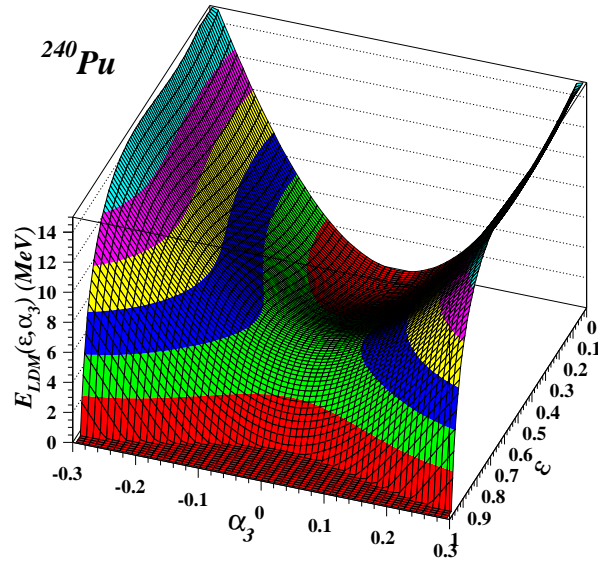


Figure 3.2: LDM deformation energy surface plot in ε and α_3 for the heavy nucleus ^{240}Pu .

with $\left(\frac{Z^2}{A}\right)_{cr} = 45$.

To account for finite-range effects, although small in the Coulomb the energy (see the middle panel of fig.3.1), we have to add the correction

$$\begin{aligned} \delta E_C^0 &= E_C^0 \left\{ -5 \left(\frac{a}{r_0}\right)^2 \left[1 - 0.375 \frac{a}{r_0} \left(5 - 7 \left(\frac{a}{r_0}\right)^2 \right) \right. \right. \\ &\quad \left. \left. - 0.75 e^{-2r_0/a} \left(1 + 4.5 \frac{a}{r_0} + 7 \left(\frac{a}{r_0}\right)^2 + 3.5 \left(\frac{a}{r_0}\right)^3 \right) \right] \right\} \end{aligned} \quad (3.22)$$

3.1.4 Deformation Energy

The macroscopic part of the deformation energy is computed according to the LDM, i.e. the actual total energy minus the value for a sphere (see [8], p.14, eq.(1.74))

$$E_{\text{LDM}} = E_{\text{surf}} - E_s^0 + E_{\text{Coul}} - E_c^0 \quad (3.23)$$

One of the most convenient parametrization of the nuclear surface used in the computation of the deformation energies for arbitrary distortions is the Cassini parametrization [4]. In this parametrization an axially deformed shape can be constructed in cylindrical coordinates

$$\rho = \frac{1}{\sqrt{2}} [G(x)^{1/2} - R^2(x)(2x^2 - 1) - \varepsilon R_0^2]^{1/2} \quad (3.24)$$

$$z = \frac{\text{sign}(x)}{\sqrt{2}} [G(x)^{1/2} + R^2(x)(2x^2 - 1) + \varepsilon R_0^2]^{1/2} \quad (3.25)$$

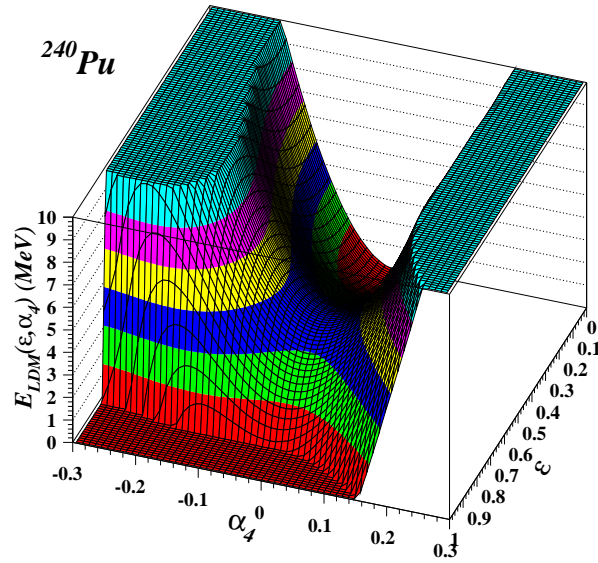


Figure 3.3: LDM deformation energy surface plot in ε and α_4 .

where

$$G(x) = [R^4(x) + 2\varepsilon R_0^2 R^2(x)(2x^2 - 1) + \varepsilon^2 R_0^4]^{1/2}$$

The curve $R(x)$ is expanded in Legendre polynomials

$$R(x) = R_0 \left(1 + \sum_m \alpha_m P_m(x) \right) \quad (3.26)$$

Thus a deformed shape in Cassini parametrization is described by the following deformation parameters: $\varepsilon, \alpha_m, m = 1, 2, \dots, M$. In the calculation of the finite-range part of the potential there is a difference compared to Krappe et al. One takes $r_0 = 1.16$ fm and $a = 0.68$ fm.

In the low panel of fig.3.1 the LDM deformation energy is plotted against ε . For reflexion-symmetrical shapes $\alpha_3 = 0$ the barrier is smaller than for reflexion-asymmetrical shapes. But the most visible feature of this plot is the tremendous decrease of the barrier when finite-range corrections are introduced.

In fig.3.2 the LDM energy surface plot is given in terms of the deformation ε , which describes symmetric elongations and α_3 , which describes octupole or reflexion-asymmetric distortions. All higher deformations are kept fixed, $\alpha_{4, \dots, 9} = 0$. Consequently the LDM predicts a symmetrical fission barrier, centered on the direction $\alpha_3 = 0$. Since the octupole deformation has similarities with the mass-asymmetry $\eta = (A_1 - A_2)/(A_1 + A_2)$ then the most favourable valley for fusion is also the symmetric one. If instead of α_3 the hexadecupole deformation α_4 is varied, keeping again fixed all other deformations $\alpha_{3, \dots, 9} = 0$ an asymmetric surface is obtained (see Fig.3.3). The lowest barriers is again encountered along $\alpha_4 = 0$.

It is important to note that models based on the incompressible liquid drop model of the nucleus lead to the correct connection between the properties of normal nuclear matter and the behavior of the interaction potential at the edge of the nucleus. At short-distances they give a weak attraction and do not have a repulsive core.

3.2 Shell Corrections

3.2.1 Phenomenological shell corrections

The phenomenological method introduced by Myers and Swiatecki [3] is a uncomplicated functional form which enables the rapid evaluation of nuclear shell corrections. It is convenient to use in the cluster decay or cold fission due to the fact that the fragments are close to their ground state deformations. The Myers-Swiatecki shell energy is expected to describe the potential energy of fragments far off the line of β stability with sufficient accuracy, as it accounts well for the binding energies and quadrupole moments of a large number of nuclei throughout the Periodic Table.

The shell correction of Myers and Swiatecki [3] for a nucleus which stands only spheroidal deformations reads

$$V_{\text{shell}} = C \left[\frac{F(N) + F(Z)}{(A/2)^{2/3}} - cA^{1/3} \right] (1 - 2\theta^2) \exp(-\theta^2) \quad (3.27)$$

where

$$F(m) = \frac{3}{5} \frac{M_i^{5/3} - M_{i-1}^{5/3}}{M_i - M_{i-1}} (m - M_{i-1}) - \frac{3}{5} (m^{5/3} - M_{i-1}^{5/3}) \quad (3.28)$$

and M_i and M_{i-1} denote the nearest(spherical) magic numbers

$$M_{i-1} \leq m \leq M_i \quad (3.29)$$

For spheroids, θ in eq.(3.27) is related to the Hill-Wheeler parameter σ [49] by

$$\theta^2 = \frac{(r_0 A^{1/3})^2 \sigma^2 (1 - \frac{1}{7}\sigma)}{5a^2} \quad (3.30)$$

and to the major semiaxis z by

$$\sigma = \ln \left(\frac{z}{r_0 A^{1/3}} \right) \quad (3.31)$$

The parameters entering in the above formula are $C=5.8$ MeV, $c=0.325$ and $a=0.444r_0$, $r_0 = 1.2249$ fm.

If the shape is non-axial($\gamma \neq 0$), but still ellipsoidal, the shell corrections can be obtained by a curvature-dependent integration [9]

$$V_{\text{shell}} = \frac{C}{4\pi r_0^2 A^{4/3}} \int k \left\{ \left[F \left(\frac{N}{k^3} \right) + F \left(\frac{Z}{k^3} \right) \right] 2^{2/3} k^3 - cA \right\} dS \quad (3.32)$$

where

$$k = 2r_0 A^{1/3} \left[\frac{1 - \alpha}{\mathcal{R}_{\parallel} + \mathcal{R}_{\perp}} + \frac{\alpha}{|S|} \int \frac{dS}{\mathcal{R}_{\parallel} + \mathcal{R}_{\perp}} \right] \quad (3.33)$$

where $\mathcal{R}_{\parallel} = 1/\kappa_{\parallel}$ and $\mathcal{R}_{\perp} = 1/\kappa_{\perp}$ are the curvature radii, the curvatures, κ^{\parallel} and κ^{\perp} , being defined in (3.144-3.145).

3.3 Folded Potential Model

The folding model of the potential between two nuclei has been used widely to generate the real parts of both α -nucleus and heavy-ion optical potentials. Antisymmetrization of the system is taken into account by considering single-nucleon 'knock-on' exchange terms in which the interacting pair of nucleons is exchanged. The success of this potential in describing the observed elastic scattering of many systems suggests that it produces the dominant part of the real optical potential [10, 11].

3.3.1 Microscopical Foundations

Although there is presently no microscopic theory for the nucleus-nucleus scattering, a microscopical foundation of the optical potential for the scattering of two composite nuclei is available within the framework of the Feshbach theory of nuclear reactions [12].

If the exchange of nucleons due to antisymmetrization is initially ignored then the total wavefunction for the colliding projectile (p) plus target (t) system, may be expanded in terms of the complete set of internal eigenstates of the individual nuclei

$$\Psi = \sum_{ij} \mathcal{R}_{ij}(\mathbf{r}) \phi_{pi}(\xi_p) \phi_{tj}(\xi_t) \quad (3.34)$$

where \mathcal{R}_{ij} describes the relative motion when the nuclei are in their internal states labelled i and j . If $i = 0$ and $j = 0$ denotes the ground states of the nuclei, then the radial wavefunction component \mathcal{R}_{00} gives the elastic scattering. The problem is to find an effective interaction, or optical potential, U_E that will generate \mathcal{R}_{00} when plugged in the one-body Schrödinger equation

$$\left[-\frac{\partial \hbar^2}{2\mu} \nabla^2 + U_E(r) \right] \mathcal{R}(\mathbf{r}) = E \mathcal{R}(\mathbf{r}) \quad (3.35)$$

In the Feshbach theory the Hilbert space is partitioned into the prompt (the first state) \mathcal{P} and delaying (the second state) \mathcal{D} components which are orthogonal. The open channels (resonant states) are included usually in \mathcal{P} and the closed channels in \mathcal{D} . Suppose that \mathcal{P} consists only of the elastic channel χ_{00} . Feshbach introduced projection operators P and Q onto the spaces \mathcal{P} and \mathcal{D} . Writing (3.34) in the form

$$\Psi = P \Psi + Q \Psi \quad (3.36)$$

where

$$P \Psi = \mathcal{R}_{00}(\mathbf{r}) \phi_{p0}(\xi_p) \phi_{t0}(\xi_t), \quad Q \Psi = \sum_{i,j \neq 0,0} \mathcal{R}_{ij}(\mathbf{r}) \phi_{pi}(\xi_p) \phi_{tj}(\xi_t) \quad (3.37)$$

and introducing the notations

$$H_{00} \equiv PHP, \quad H_{0n} \equiv PHQ, \quad H_{n0} \equiv QHP, \quad H_{nn} \equiv QHQ, \quad (3.38)$$

where the label 0 stands for the ground state and n for the closed channels, and multiplying the many-body Schrödinger equation satisfied by Ψ

$$(E - H) \Psi = E \Psi \quad (3.39)$$

from the left by P and Q we obtain

$$(E - H_{00})(P\Psi) = H_{0n}Q\Psi, \quad (E - H_{QQ})(Q\Psi) = H_{n0}P\Psi \quad (3.40)$$

Since the many-body Hamiltonian $H = H_0 + V$ is the sum of the Hamiltonians for the internal degrees of freedom of the projectile and target and the kinetic energy operator for their relative motion (H_0) and the potential (V), Feshbach restricts the class of projection operators to those for which

$$H_{0n} = V_{0n} \quad H_{n0} = V_{n0} \quad (3.41)$$

The coupled Feshbach equations (3.40) can be formally solved as follows:

$$Q\Psi = \lim_{\eta \rightarrow 0} \left(\frac{1}{E - H + i\eta} \right)_{nn} V_{n0} P\Psi \quad (3.42)$$

The above expression includes the boundary condition that there is no incident wave in the subspace D . The $i\eta$ in the denominator of (3.42) is introduced in case some of the open channels are included in D . Substituting (3.42) the first equation from (3.40) yields

$$(E - H_0 - U_E)P\Psi = 0 \quad (3.43)$$

where

$$U_E = V_{00} + \lim_{\eta \rightarrow 0} V_{0n} \left(\frac{1}{E - H_{00} + i\eta} \right)_{nn} V_{n0} \quad (3.44)$$

The separation of the radial part in (3.43) leads to the desired equation (3.35). The first term in the effective interaction (3.44), V_{00} , is associated with the prompt(elastic) process and it is simply the folded potential

$$V_{00} = V_F(r) \equiv \langle \phi_{p0} \phi_{t0} | V | \phi_{p0} \phi_{t0} \rangle \quad (3.45)$$

where V is the (real) interaction between the two nuclei. The second term describes the time-delaying effect of coupling the elastic channel (space \mathcal{P}) with the channels from space \mathcal{D} , propagation in \mathcal{D} as given by $(1/E - H_{00} + i\eta)_{nn}$ and then reemission into \mathcal{P} . It is often denoted in the literature by ΔU_E and referred as the *dynamic polarization potential*(DPP). We see that ΔU_E is energy dependent, complex and nonlocal. These properties are consequences of the presence of the propagator $(1/E - H_{00} + i\eta)_{nn}$. The imaginary part arises from energy-conserving transitions to open nonelastic channels in which flux is lost from the elastic channel. The real part comes from virtual excitations, corresponding to readjustment of the two nuclei when they began to interact but which are reversed and they return to their ground states. Energetically closed channels can contribute to the real part of ΔU_E . The dispersion relation between the real and imaginary part of ΔU_E is derived in [12]. Nonlocality of ΔU_E means that if the system is excited into a nonelastic channel at position \mathbf{r} , then it will in general return to the elastic channel at another position $\mathbf{r}' \neq \mathbf{r}$.

It is assumed that the interaction V is a sum of local two-body potentials

$$V = \sum_{pt} v_{pt} \quad (3.46)$$

with p labelling a nucleon in the projectile and t one in the target,

The individual internal wave functions $\phi_{p(t)i}(\xi)$ in (3.34) are each taken to be antisymmetrized. Since the Pauli principle requires that the total wavefunction Ψ must also be antisymmetric under interchange of nucleons between the two nuclei, the so-called *knock-on exchange* term is introduced in v_{pt}

$$v_{pt} \rightarrow v_{pt}(1 - P_{pt}) \quad (3.47)$$

where P_{pt} is the operator that exchanges all coordinates of these two nucleons. In a collision the knock-on exchange results in a target nucleon being ejected and replaced by the projectile nucleon following their mutual interaction. Consequently the first term of the effective potential (3.44) is replaced in this approximation by

$$V_{00} = V_F(r) \equiv \langle \phi_{p0}\phi_{t0} | \sum_{pt} v_{pt}(1 - P_{pt}) | \phi_{p0}\phi_{t0} \rangle \quad (3.48)$$

By interchanging the spatial positions of the two nucleons the centres of mass of the two nuclei are affected together with their separation distance $\mathbf{r}' \neq \mathbf{r}$. The corresponding exchange contribution to the potential V_{00} becomes nonlocal.

3.3.2 Double-Folding Integral

Consider two heavy ions with one-body ground-state deformed densities ρ_1 and ρ_2 and center of masses separated by the distance \mathbf{R} . Then the interaction (3.48) between these two ions can be evaluated as the double folding integral of these densities

$$V(\mathbf{R}) = \langle \phi_{10}\phi_{20} | V | \phi_{10}\phi_{20} \rangle = \int d\mathbf{r}_1 \int d\mathbf{r}_2 \rho_1(\mathbf{r}_1)\rho_2(\mathbf{r}_2)v(\mathbf{r}_{12}, \rho_1, \rho_2) \quad (3.49)$$

where $\mathbf{r}_{12} = \mathbf{R} + \mathbf{r}_2 - \mathbf{r}_1$. For simplicity, the spin and isospin was ignored. In the above formula there is allowance for a possible density dependence of v .

The evaluation of the above folding integral is facilitated by the convolution theorem which states that the Fourier transform of the folded quantity is simply the product of the transforms of the individual component functions [14, 15]. Introducing the Fourier transform $\tilde{V}(\mathbf{q})$ of the double-folding integral (3.49) through

$$\tilde{V}(\mathbf{q}) = \int d\mathbf{r} \exp(i\mathbf{q} \cdot \mathbf{R})V(\mathbf{R}) \quad (3.50)$$

the double-folding integral (3.49) writes

$$V(\mathbf{R}) = (2\pi)^{-3} \int d\mathbf{q} \tilde{V}(\mathbf{q}) \exp(-i\mathbf{q} \cdot \mathbf{R}) \quad (3.51)$$

where the Fourier transform of the double-folding potential reads

$$\tilde{V}(\mathbf{q}) = \tilde{\rho}_1(\mathbf{q})\tilde{\rho}_2(-\mathbf{q})\tilde{v}(\mathbf{q}) \quad (3.52)$$

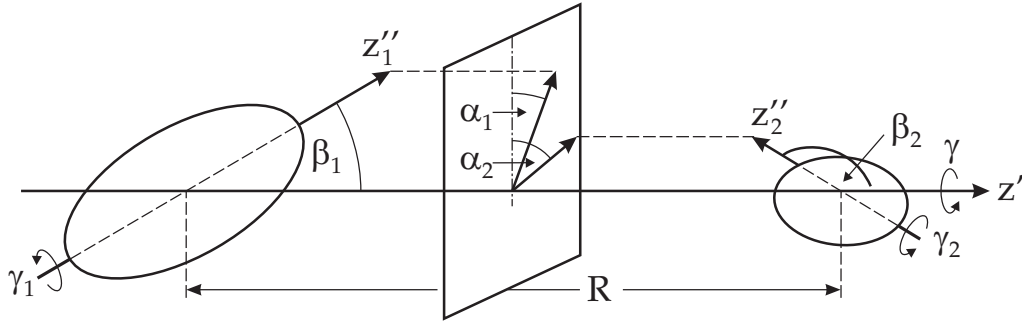


Figure 3.4: The position and space orientation of the two nuclei is described by the center-to-center distance and the Euler angles $\alpha_i, \beta_i, \gamma_i$ which are giving the transformation to the intrinsic system.

Consider the geometry from Figure 3.4, where the unprimed axis corresponds to the laboratory frame, the primed to the molecular (dinuclear system) frame and the double primed to the body fixed framed of each nucleus. The density distribution $\rho_i(\mathbf{r}')$ in the molecular frame is related to that in the body-fixed frame by Euler rotations

$$\rho_i(\mathbf{r}') = \mathcal{R}(\alpha_i, \beta_i, \gamma_i) \rho_i(\mathbf{r}'') \quad (3.53)$$

In the above formula we adopted for each set of Euler angles, $(\alpha_i, \beta_i, \gamma_i)$, the condensed notation ω_i . We consider that the density distributions in the principal axes, $\rho_i(\mathbf{r}'')$, is axial symmetric

$$\rho_i(\mathbf{r}'') = \sum_{\lambda} \rho(r''_{\lambda}) Y_{\lambda 0}(\hat{r}''_{\lambda}) \quad (3.54)$$

and that its shape is given by a Fermi distribution

$$\rho_i(\mathbf{r}'') = \frac{\rho_0}{1 + e^{\frac{r''_{\lambda} - c_i}{a}}} \quad (3.55)$$

with $c_i = c_0(1 + \sum_{\lambda \geq 2} \beta_{\lambda} Y_{\lambda 0}(\hat{r}''_{\lambda}))$. The constant ρ_0 is fixed by normalizing the proton and neutron density to the Z_i proton and N_i neutron numbers, respectively. This condition ensures the volume conservation. The half radius c_0 and the diffusivity a are taken from the liquid drop model [16].

Using the transformation property of the spherical harmonics under Euler rotations [17]

$$\mathcal{R}(\omega_i) Y_{lm'}(\theta, \phi) = \sum_m Y_{lm}(\theta, \phi) D_{mm'}^l(\omega_i) \quad (3.56)$$

we obtain for the density distribution in the molecular frame

$$\rho(\mathbf{r}'_i) = \sum_{\lambda\mu} \rho_{\lambda}(r_i) D_{\mu 0}^{\lambda}(\omega_i) Y_{\lambda\mu}(\hat{r}'_i) \quad (3.57)$$

The Fourier transform of the density distribution $\tilde{\rho}(\mathbf{q}) = \int d\mathbf{r} \rho(\mathbf{r}) \exp(i\mathbf{q} \cdot \mathbf{r})$, occurring in (3.52), can be calculated using the plane wave expansion

$$\exp(i\mathbf{q} \cdot \mathbf{r}) = 4\pi \sum_{lm} i^l j_l(qr) Y_{lm}^*(\Omega_q) Y_{lm}(\hat{r}') \quad (3.58)$$

which leads to the final expression

$$\tilde{\rho}(\pm\mathbf{q}) = 4\pi \sum_{\lambda\mu} (\pm i)^\lambda D_{\mu 0}^\lambda(\omega_i) Y_{\lambda\mu}(\Omega_q) \tilde{\rho}_\lambda(q) \quad (3.59)$$

where

$$\tilde{\rho}_\lambda(q) = 4\pi \int dr r^2 \rho_\lambda(r) j_\lambda(qr) \quad (3.60)$$

The Fourier transform of the nucleon-nucleon interaction reads

$$\tilde{v}(\mathbf{q}) = \int d\mathbf{s} v(\mathbf{s}) \exp(i\mathbf{q} \cdot \mathbf{s}) = 4\pi \int dr s^2 j_0(qs) v(s) \quad (3.61)$$

The Fourier transform of the double-folding potential (3.52) reads

$$\tilde{V}(\mathbf{q}) = \sum_{\lambda_1\mu_1} \sum_{\lambda_2\mu_2} i^{\lambda_1-\lambda_2} D_{\mu_1 0}^{\lambda_1}(\omega_1) D_{\mu_2 0}^{\lambda_2}(\omega_2) Y_{\lambda_1\mu_1}(\Omega_q) Y_{\lambda_2\mu_2}(\Omega_q) \tilde{\rho}_{\lambda_1}(q) \tilde{\rho}_{\lambda_2}(q) \tilde{v}(q) \quad (3.62)$$

which substituted in (3.51) leads to the following expression of the double-folding potential (3.49) in multipolar form

$$\begin{aligned} V(\mathbf{R}) &= \frac{1}{(2\pi)^3} \sum_{\lambda_i\mu_i} i^{\lambda_1-\lambda_2-\lambda_3} \hat{\lambda}_1 \hat{\lambda}_2 \hat{\lambda}_3^2 \begin{pmatrix} \lambda_1 & \lambda_2 & \lambda_3 \\ 0 & 0 & 0 \end{pmatrix} \begin{pmatrix} \lambda_1 & \lambda_2 & \lambda_3 \\ \mu_1 & \mu_2 & \mu_3 \end{pmatrix} \\ &\times D_{\mu_1 0}^{\lambda_1}(\omega_1) D_{\mu_2 0}^{\lambda_2}(\omega_2) D_{\mu_3 0}^{\lambda_3}(\Phi, \Theta, 0) F_{\lambda_1\lambda_2\lambda_3}(R) \end{aligned} \quad (3.63)$$

with the radial part given by the oscillating integral

$$F_{\lambda_1\lambda_2\lambda_3}(R) = \int dq q^2 \tilde{\rho}_{\lambda_1}(q) \tilde{\rho}_{\lambda_2}(q) j_{\lambda_3}(qR) \tilde{v}(q) \quad (3.64)$$

Above Φ, Θ are giving the orientation of the molecular system with respect to the molecular axis. Then eq.(3.63) can be rewritten in the more condensed form in which the radial and angular parts are factorizing

$$V(\mathbf{R}) = \sum_{\lambda_i\mu_i} V_{\lambda_1 \lambda_2 \lambda_3}^{\mu_1 \mu_2 \mu_3}(R) D_{\mu_1 0}^{\lambda_1}(\omega_1) D_{\mu_2 0}^{\lambda_2}(\omega_2) D_{\mu_3 0}^{\lambda_3}(\Phi, \Theta, 0) \quad (3.65)$$

The radial multipoles are writing

$$V_{\lambda_1 \lambda_2 \lambda_3}^{\mu_1 \mu_2 \mu_3}(R) = \frac{1}{(2\pi)^3} i^{\lambda_1-\lambda_2-\lambda_3} \hat{\lambda}_1 \hat{\lambda}_2 \hat{\lambda}_3^2 \begin{pmatrix} \lambda_1 & \lambda_2 & \lambda_3 \\ 0 & 0 & 0 \end{pmatrix} \begin{pmatrix} \lambda_1 & \lambda_2 & \lambda_3 \\ \mu_1 & \mu_2 & \mu_3 \end{pmatrix} F_{\lambda_1\lambda_2\lambda_3}(R) \quad (3.66)$$

If the fission(molecular)-axis is fixed in the laboratory frame, then one can chose $\Theta = \Phi = 0$, and $D_{\mu_3 0}^{\lambda_3}(\Phi, \Theta, 0) = \delta_{\mu_3 0}$ which leads to:

$$\begin{aligned}
V(\mathbf{R}) &= \sum_{\lambda_i \mu} V_{\lambda_1 \lambda_2 \lambda_3}^{\mu -\mu \ 0}(R) D_{\mu 0}^{\lambda_1}(\alpha_1, \beta_1, 0) D_{-\mu 0}^{\lambda_2}(\alpha_2, \beta_2, 0) \\
&= \frac{1}{2} \sum_{\lambda_i \mu} V_{\lambda_1 \lambda_2 \lambda_3}^{\mu -\mu \ 0}(R) (1 + (-)^{\lambda_1 + \lambda_2 - \lambda_3}) \cos \mu(\alpha_2 - \alpha_1) d_{\mu 0}^{\lambda_1}(\beta_1) d_{-\mu 0}^{\lambda_2}(\beta_2) \\
&+ \frac{1}{2} \sum_{\lambda_i \mu} V_{\lambda_1 \lambda_2 \lambda_3}^{\mu -\mu \ 0}(R) (1 - (-)^{\lambda_1 + \lambda_2 - \lambda_3}) \sin \mu(\alpha_2 - \alpha_1) d_{\mu 0}^{\lambda_1}(\beta_1) d_{-\mu 0}^{\lambda_2}(\beta_2)
\end{aligned} \tag{3.67}$$

Due to the 3- j coefficient occuring in eq.(3.66) with all the angular momentum projections equal to zero, the angular momenta must fulfill $\lambda_1 + \lambda_2 - \lambda_3 = \text{even}$, otherwise the 3- j equals zero. Thence, the last line in the eq.(3.67) cancels and the final expression of the double-folding potential reads

$$V(\mathbf{R}) = \sum_{\lambda_i \mu} V_{\lambda_1 \lambda_2 \lambda_3}^{\mu -\mu \ 0}(R) \cos \mu(\alpha_2 - \alpha_1) d_{\mu 0}^{\lambda_1}(\beta_1) d_{-\mu 0}^{\lambda_2}(\beta_2) \tag{3.68}$$

3.3.3 Effective $N - N$ Interaction

The central part of the effective $N - N$ potential interaction v may be written

$$\begin{aligned}
v &= v_{00}(\mathbf{r}_{12}) + v_{01}(\mathbf{r}_{12}) \boldsymbol{\tau}_1 \cdot \boldsymbol{\tau}_2 + v_{10}(\mathbf{r}_{12}) \boldsymbol{\sigma}_1 \cdot \boldsymbol{\sigma}_2 + v_{11}(\mathbf{r}_{12}) (\boldsymbol{\tau}_1 \cdot \boldsymbol{\tau}_2) \cdot (\boldsymbol{\sigma}_1 \cdot \boldsymbol{\sigma}_2) \\
&+ (v_0^{LS} + v_1^{LS} \boldsymbol{\tau}_1 \cdot \boldsymbol{\tau}_2) \mathbf{L}_{12} \cdot (\boldsymbol{\sigma}_1 + \boldsymbol{\sigma}_2) \\
&+ (v_0^T + v_1^T \boldsymbol{\tau}_1 \cdot \boldsymbol{\tau}_2) S_{12}
\end{aligned} \tag{3.69}$$

where \mathbf{s} , $\boldsymbol{\tau}$ are the Pauli matrices for spin and isospin respectively. The first row of the above equations represents the central part of the effective potential. The second row contains the spin-orbit (LS) part where the relative angular momentum is

$$\mathbf{L}_{12} = \frac{1}{2\hbar} (\mathbf{r}_1 - \mathbf{r}_2) \times (\mathbf{p}_1 - \mathbf{p}_2) \tag{3.70}$$

and the third row the tensor term (T) where the tensor operator is

$$S_{12} = 3(\boldsymbol{\sigma}_1 \cdot \hat{\mathbf{r}}_{12})(\boldsymbol{\sigma}_2 \cdot \hat{\mathbf{r}}_{12}) - \boldsymbol{\sigma}_1 \cdot \boldsymbol{\sigma}_2 \tag{3.71}$$

In our next considerations we drop-out the non-central terms.

When either target or projectile has zero spin, the central term $v_{11}(\mathbf{r}_{12}) (\boldsymbol{\tau}_1 \cdot \boldsymbol{\tau}_2) \cdot (\boldsymbol{\sigma}_1 \cdot \boldsymbol{\sigma}_2)$ with $S = 1$ do not contribute. Similarly it will not contribute when $T = 1$ if either nucleus has zero isospin ($N = Z$). Usually the spin terms are relativey unimportant in barrier penetration phenomena. Only one or a few unpaired nucleons in each nucleus contribute to the $S = 1$ potential whereas all nucleons contribute to the $S = 0$ potential. Also the $T = 1$ interactions tend to make a small contribution.

For two spinless nuclei ($S=0$) the integrand of the double folding integral (3.49) may be written

$$\rho_1 \rho_2 v_{00} + (\rho_1^n - \rho_2^p)(\rho_1^n - \rho_2^p) v_{01} \quad (3.72)$$

where $\rho_i^{n(p)}$ are the neutron(proton) distributions in nucleus i . In all the calculations we assume that $\rho_i^n = (N_i/A_i)\rho_i$ and $\rho_i^p = (Z_i/A_i)\rho_i$ and (3.72) rewrites

$$\rho_1 \rho_2 \left[v_{00} + v_{01} \frac{(N_1 - Z_1)(N_2 - Z_2)}{A_1 A_2} \right] \quad (3.73)$$

For realistic interactions v_{01} and v_{00} are comparable (typically $v_{01}/v_{00} \approx -0.5$). For usual light quasi-molecular systems such as $^{12}\text{C}-^{12}\text{C}$, $^{28}\text{Si}-^{28}\text{Si}$, $^{56}\text{Ni}-^{56}\text{Ni}$, the asymmetry $(N_i - Z_i)/A_i$ is zero. It is obvious that this term is important only in case of very neutron-rich targets and projectiles. In the cold fission of ^{252}Cf the fragments are in average moderately neutron rich. In the splitting $^{252}\text{Cf} \rightarrow ^{106}\text{Mo} + ^{146}\text{Ba}$ we have that $(N_1 - Z_1)/A_1 \approx 0.21$ and $(N_2 - Z_2)/A_2 \approx 0.23$ which gives a contribution of up to 2.5% in the double folding integrand. Since such a contribution to the fission(fusion) can give a sensitive change in the transmission probabilities this term is taken into account throughout our calculations. Thus in this work only the isoscalar and isovector components have been retained. The spin-dependent components have been neglected since for a lot of fragments involved in the calculation the ground state spins are unknown. Moreover, the spin-spin component of the heavy-ion potential is of the order $1/A_1 A_2$ and can be safely neglected for heavy and superheavy nuclei.

As discussed above the only effect of antisymmetrization under exchange of nucleons between the two nuclei that is normally included in the folding model is the single-nucleon knock-on exchange in which the two nucleons that are interacting via v_{pt} are interchanged. As concluded in [18] the knock-on exchange potential can be estimated quite accurately by adding a zero-range pseudo-potential to the interaction v_{pt}

$$v'_{pt} = v_{pt}(1 - P_{tp}) \rightarrow v_{pt} + \hat{J}(E)\delta(\mathbf{r}_{pt}) \quad (3.74)$$

By introducing the delta function, i.e. a zero-range force, the exchange term becomes local. The strength depends weakly on the energy E .

Density-independent M3Y interaction

Among the effective $N - N$ interactions introduced into the folding model, the Michigan-3 Yukawa (M3Y) parametrization is one of the most widely used. Details about the derivation are given in [19]. This interaction is particularly simple to use in folding models since it is parametrized as a sum of 3 Yukawa functions in each spin-isospin (S, T) channel.

The explicit form of the central term appearing in (3.69) is given in the versions Reid and Paris

$$v_{00}(r) = \left[7999 \frac{e^{-4r}}{4r} - 2134 \frac{e^{-2.5r}}{2.5r} \right] \text{ MeV,} \quad \text{M3Y - Reid} \quad (3.75)$$

$$v_{00}(r) = \left[11062 \frac{e^{-4r}}{4r} - 2538 \frac{e^{-2.5r}}{2.5r} \right] \text{ MeV,} \quad \text{M3Y - Paris} \quad (3.76)$$

Both versions consists of a short-ranged repulsion and a long-ranged attraction, passing through zero near $r \approx 0.5$ fm. In momentum space the the equation $v_{00}(q) = 0$ has a solution at $q \approx 2$ fm⁻¹.

The folding integral (3.49) satisfies some simple relations if v_{pt} does not depend upon the densities. If the density distributions are spherically symmetric and v_{pt} is scalar, then

$$J(V) = J(v)J(\rho_1)J(\rho_2) = A_1A_2J(v) \quad (3.77)$$

where J is the "volume integral" of the function f

$$J(f) = 4\pi \int f(r)r^2dr \quad (3.78)$$

Furthermore, the mean-square radii are introduced

$$\langle r^2 \rangle_V = \langle r^2 \rangle_1 + \langle r^2 \rangle_2 + \langle r^2 \rangle_{12} \quad (3.79)$$

where

$$\langle r^2 \rangle_f = \frac{\int dr r^4 f(r)}{\int dr r^2 f(r)} \quad (3.80)$$

Then, the volume integrals of the interactions (3.76) and (3.76) are $J_{00}(\text{Reid})=-146$ MeV fm³ and $J_{00}(\text{Paris})=+131$ MeV fm³. The mean-square radius for the Reid version is 7.6 fm², while for the Paris version it is 8.73 fm²

The M3Y interaction is dominated by the exchange component, therefore it is extremely important to include this component in the barrier calculation in an accurate way. The one-nucleon knock-on exchange term leads to a nonlocal kernel. The range of the nonlocality behaves as μ^{-1} , where $\mu = A_1A_2/(A_1 + A_2)$ is the reduced mass of the interacting system, and therefore the nonlocal potential is reduced in the present case to a zero range pseudopotential $\hat{J}_{00}\delta(s)$, with a strength depending slightly on the energy. The magnitude of \hat{J}_{00} has been determined empirically [20] by comparing cross sections for proton scattering from various targets, and at various energies up to 80 MeV, calculated using (3.74) with those in which the exchange was calculated exactly. The results for boths versions(Reid and Paris) can be expressed as

$$\hat{J}_{00} \approx -276 [1 - 0.005(E/A)] \text{ MeV} \quad (\text{M3Y} - \text{Reid}) \quad (3.81)$$

$$\hat{J}_{00} \approx -590 [1 - 0.002(E/A)] \text{ MeV} \quad (\text{M3Y} - \text{Paris}) \quad (3.82)$$

where E/A is the bombarding energy per projectile nucleon in MeV. In cold process the energy is not high and therefore we neglect the energy dependence. For example, the odd-even staggering in the Q -value for a fragmentation channel, which is typically of the order $\Delta Q=2$ MeV, leads to a variation with $\Delta \hat{J}_{00}=-0.005\Delta Q/\mu$ MeV·fm³ with $\mu \approx 100$. In treating the exchange potential of the α -nucleus and light-ions scattering a finite-range was proposed [21]

$$v_{00}^{ex}(r) = \left[4631 \frac{e^{-4r}}{4r} - 1787 \frac{e^{-2.5r}}{2.5r} - 7.847 \frac{e^{-0.7072r}}{0.7072r} \right] \text{ MeV}, \quad \text{M3Y} - \text{Reid} \quad (3.83)$$

$$v_{00}^{ex}(r) = \left[-1524 \frac{e^{-4r}}{4r} - 518.8 \frac{e^{-2.5r}}{2.5r} - 7.847 \frac{e^{-0.7072r}}{0.7072r} \right] \text{ MeV}, \quad \text{M3Y} - \text{Paris} \quad (3.84)$$

An important difference between the Reid-based and Paris-based direct interactions is that the later is repulsive. Its volume integral is comparable in magnitude to the Reid one, but of opposite sign. On the other hand, the Paris exchange term is roughly twice as attractive as the Reid one. This fact becomes transparent by inspecting the pseudo-potential strengths (3.81) and (3.82). However when direct and exchange potentials are combined, their sums are very similar [22].

For the Reid version of the central isovector part the following form is used

$$v_{01}(r) = \left[-4885.5 \frac{e^{-4r}}{4r} + 1175.5 \frac{e^{-2.5r}}{2.5r} \right] \text{ MeV} \quad (3.85)$$

and for the isovector component of the knock-on exchange term

$$\hat{J}_{01} = 217 \text{ MeVfm}^3 \quad (3.86)$$

Taking into account only the isoscalar and isovector components the effective density-independent $N - N$ interaction used in this work is

$$v(\mathbf{r}_{12}) = v_{00}(\mathbf{r}_{12}) + \hat{J}_{00}\delta(\mathbf{r}_{12}) + (v_{01}(\mathbf{r}_{12}) + \hat{J}_{01}\delta(\mathbf{r}_{12}))\boldsymbol{\tau}_1 \cdot \boldsymbol{\tau}_2 \quad (3.87)$$

It is important to remark that the M3Y forces are purely real, so that the imaginary part of the optical potential either has to be constructed independently or treated phenomenologically.

A second remark is that they are independent of the density of nuclear matter in which the nucleons are embedded, and are also independent of energy except for the weak dependence of the knock-on exchange.

Density-dependent M3Y interaction

The density dependence of the effective $N - N$ interaction in a nucleus is required for nuclear matter to saturate rather than to collapse. Folded potentials based upon density-independent interactions like the M3Y are able to reproduce the data on α scattering at forward angles or low energies. Thus, the potential experienced in peripheral collisions is correctly reproduced. However, the rainbow-like features seen at high energies and larger angles were not reproduced because these features are sensitive to the real potential at smaller radii. This drawback stems from the fact that the folded potential is at least a factor of two to deep. This is a clear indication that the effective interaction must depend upon the position within the nucleus of the two interacting nucleons.

A density dependence is introduced in the M3Y(DDM3Y) interaction assuming that the effective N-N interaction factorizes in a radial part independent of the energy and a factor dependent on energy and density [11]

$$v^{DD}(\rho, E, r) = f(\rho, E)v'(r) \quad (3.88)$$

where $v'(r)$ is the original M3Y interaction(including the knock-on pseudo-potential). Although this factorization is rather arbitrary from theoretical point of view, the approximation

that the shape of $v(r)$ does not vary strongly with density at low bombarding energies is reasonable. According to ref.[23] the density-dependent factor is taken in the form

$$f(\rho, E) = C(E) [1 + \alpha(R)e^{-\beta(E)\rho}] \quad (3.89)$$

with

$$\rho = \rho_1(r_1) + \rho_2(r_2) \quad (3.90)$$

The parameters $C(E)$, $\alpha(E)$ and $\beta(E)$ are chosen at each energy so as to make the variation with density of the volume integral of v^{DD} match as well as possible the results of the Bruckner-type calculations for a nucleon scattering from nuclear matter at various densities ρ ranging from about 5% to 100% of normal nuclear matter and at nucleon energies from 10 to 140 MeV [24].

Then the isoscalar part of the DDM3Y interaction is

$$v_{00}^{DDM3Y}(\rho, E, r; \text{Reid}) = f(\rho, E) [v_{00}(r; \text{Reid}) + \hat{J}_{00}(E; \text{Reid})\delta(r)] \quad (3.91)$$

A difficulty related to the density dependent Ansatz (3.89) is the occurrence of densities roughly twice that of normal matter, $\rho \approx 2\rho_0$, when the two ions are overlapping. The main problem is that different versions of the density dependence give, by design, the same saturation properties but different curvatures of the binding energy curve $B(\rho)$ near the saturation point, i.e. they are associated with different values of the nuclear incompressibility

$$K = 9\rho^2 \frac{d^2 B(\rho)}{d\rho^2} \quad (3.92)$$

Although the DDM3Y interaction insures the saturation of the binding energy per nucleon, $B(\rho \ll \rho_0)$ at large overlap (about 16 MeV per nucleon), it provides a wrong minimum of the normal density at $\rho_0 \approx 0.07 \text{ fm}^{-3}$ instead of $\rho_0 \approx 0.17 \text{ fm}^{-3}$ as predicted by Hartree-Fock approximation of the nuclear matter. Consequently the conventional DDM3Y does not satisfy the criterion of saturation at the right density.

Consequently a more realistic power-law dependence on ρ [25] was adopted

$$f(\rho) = C(1 - \alpha\rho^\beta) \quad (3.93)$$

which can change sign at large ρ . The power β is taken to be one-third of an integer, corresponding to the dependence upon an integer power of the Fermi momentum. Various β were chosen ($\beta = \frac{2}{3}, 1, 2$ and 3) in combination with M3Y-Reid or M3Y-Paris. However, integer values of β allow for a simple separation of variables when these interactions are used to compute double-folded potentials. Values for C and α were selected such as to satisfy the saturation conditions $B_0 = 16 \text{ MeV}$ and $\rho_0 = 0.17 \text{ fm}^{-3}$. These new density dependent interactions were named BDM3Y [22].

The folding model for the scattering of two nuclei takes ρ to be the superposition of the target and projectile densities, such that the total density ρ approaches $2\rho_0$ when the nuclei overlap strongly. This makes the potential at small radii sensitive to the kind of density dependence assumed. The interaction in this region weakens as n (or β) increases, thereby offering the opportunity to determine the appropriate values of these two parameters whenever the scattering is sensitive to the depth of the potential in the interior. It was thus possible

Table 3.1: Parameters of the density dependencies favoured DDM3Y1 and BDM3Y1 ($n=1$) interactions, and the corresponding nuclear matter compressibilities K [22]

Interaction	C	α	β	K (MeV)
BDM3Y1-Paris	1.2521	1.7452 fm ²	1.0	270
BDM3Y1-Reid	1.2253	1.5124 fm ²	1.0	232
DDM3Y1-Paris	0.2963	3.7321	3.7384 fm ²	176
DDM3Y1-Reid	0.2845	3.6391	2.9605 fm ²	171

to evaluate the incompressibility K in α -particle-nucleus systems by Khoa et al.[22], the values summarized in Table I giving the most credible results. The parameters that describe the corresponding density dependencies of these interactions are summarized in Table 3.1. From the inspection of the results listed in this table we see for example that for complete overlap, the BDM3Y1(Paris) interaction is reduced in strength by a factor of $f(2\rho_0)/f(\rho_0) = 0.407$. This factor becomes 0.433 for the DDM3Y1 (Paris) interaction, which means that the heavy-ion interaction is roughly halved by the density dependence when they completely overlap.

This table shows also that that the DDM3Y-type $f(\rho)$ can be used to generate only low K values, which are corresponding to a nuclear equation of state (EOS) that is quite soft, while the BDM3Y-type $f(\rho)$ can be used to generate K values higher than 200 MeV. In the past it was thought that a very soft EOS is sufficient to explain the prompt explosions in supernovas, but more recent numerical studies indicate that this is not the case. The choice of 270 MeV as provided by the BDM3Y still corresponds to a soft EOS but is in satisfactory agreement with a recent determination of $K(=290 \pm 50$ MeV) based upon the production of hard photons in heavy-ions collisions [26]. Microscopic calculations of the monopole resonances are also providing K for nuclear matter from the energies of monopole vibrations in finite nuclei. It was concluded that a compression modulus in the range 210 to 220 MeV should be expected in such studies [27].

In the present work we are interested not only in the interaction of a light ion, like the α -particle with a heavy ion but also by the interaction between two heavy or even very heavy nuclei for which the above approach to the density dependent does not necessarily apply *ad literam*. For this reason another approach is considered, although the nuclear compressibility is also playing inside a principal role.

The above analysis leads to the conclusion that the heavy ion nuclear potential should also contain a short-range repulsive core V_{cor} . This short-range repulsion is a manifestation of the Pauli principle, which prevents the overlapping of the wave functions of two composite systems of fermions. The existence of the core follows also from other existing microscopic calculations of effective local ion-ion potentials such as the resonating group method (RGM) [28] and the two-center shell model(TCSM) [29]. These approaches are leading to quantitatively different estimates of the height, radius, and diffuseness of the core,

this being due, on one side, to the theoretical approaches themselves, and on the other side, to the uncertainty in the precise knowledge about the interaction of nucleons in the nuclear medium or the properties of the nuclear matter. The actual form of the repulsive core and its intensity depend strongly on the extent to which the real collisions of heavy ions are adiabatic or sudden. A further uncertainty with regard to the core parameters is associated with the influence of the individual characteristics of the considered nuclei, including the binding energies, the shape, and the nucleon distribution.

Due to these conditions of strong uncertainty we use in this work an expeditive receipt for determining the properties of the short-range repulsive core.

As we noticed earlier a region of overlapping with doubled nucleon density is formed once the distance between the nuclei becomes less than $r = R_p + R_t$, where R_p and R_t are the nuclear radii along the scattering (fission) axis. The adding of the densities increases the energy of the nucleons in his region, and therefore increases the energy of the complete system. In the case of the complete overlapping (for $r \leq R_p + R_t$) the increase is

$$\Delta V = 2A_p [B(2\rho_0) - B(\rho_0)] \quad (3.94)$$

In order to obtain the strength of the repulsive core V_{cor} we assume that ΔV must be identified with the value of the heavy-ion interaction potential at the coordinate origin

$$\Delta V = V_{cor}(0) + V_N(0) \quad (3.95)$$

where the Coulomb force is neglected. Then, in the low-energy limit we can write

$$2A_p [B(2\rho_0) - B(\rho_0)] = V_{cor} + V_N(0) \quad (3.96)$$

From the definition of the compressibility (3.92) and expanding the binding energy around the equilibrium value ρ_0

$$B(2\rho_0) - B(\rho_0) \approx \frac{1}{2}\rho_0^2 \frac{d^2 B(\rho)}{d\rho^2} \quad (3.97)$$

we obtain the following rough estimate for the height of the repulsive core for total overlap, i.e. $R = 0$

$$V_{cor} + V_N(0) \approx A_p \frac{1}{9} K \quad (3.98)$$

Similar receipts to introduce a repulsive core can be found in the literature [30]. They are based on the knowledge of the equation of state and on the requirement that for a total overlap of two nuclei a double density of the nuclear matter is obtained. The compressibility for cold nuclear matter as a function of the relative neutron excess $\delta = (\rho_n - \rho_p)/\rho$ was taken from the Thomas-Fermi model [31].

It should be noted that raising the collision energy the effect of the Pauli principle will be weakened.

The repulsive Migdal interaction

A double folding potential based on the effective Skyrme interaction is also choice for simulating a repulsive core in a two heavy-ion systems [32]. In this case the nuclear potential

between two heavy ions contains an attractive part and a repulsive one. Neglecting the spin dependence, it can be written as

$$V_N(\mathbf{R}) = C_0 \left\{ \frac{F_{in} - F_{ex}}{\rho_{00}} ((\rho_1^2 * \rho_2)(\mathbf{R}) + (\rho_1 * \rho_2^2)(\mathbf{R})) + F_{ex}(\rho_1 * \rho_2)(\mathbf{R}) \right\} \quad (3.99)$$

where $*$ denotes the convolution of two functions f and g , i.e. $(f * g)(\mathbf{x}) = \int f(\mathbf{x}')g(\mathbf{x} - \mathbf{x}')d\mathbf{x}'$ and

$$F_{in,ex} = f_{in,ex} + f'_{in,ex} \frac{N_1 - Z_1}{A_1} \frac{N_2 - Z_2}{A_2} \quad (3.100)$$

The set of parameters $C_0 = 300 \text{ MeV fm}^3$, $f_{in}=0.09$, $f_{ex}=-2.59$, $f'_{in}=0.42$, and $f'_{ex}=0.54$ are taken from Ref. [33]. To solve this integral we consider the inverse Fourier transform

$$V_N(\mathbf{R}) = \int e^{-i\mathbf{q}\cdot\mathbf{R}} \tilde{V}_N(\mathbf{q}) d\mathbf{q} \quad (3.101)$$

where the Fourier transform of the local Skyrme potential $\tilde{V}_N(\mathbf{q})$ can be casted in the form

$$\tilde{V}_N(\mathbf{q}) = C_0 \left\{ \frac{F_{in} - F_{ex}}{\rho_{00}} (\tilde{\rho}_1^2(\mathbf{q})\tilde{\rho}_2(-\mathbf{q}) + \tilde{\rho}_1(\mathbf{q})\tilde{\rho}_2^2(-\mathbf{q})) + F_{ex}\tilde{\rho}_1(\mathbf{q})\tilde{\rho}_2(\mathbf{q}) \right\} \quad (3.102)$$

Here $\tilde{\rho}(\mathbf{q})$ and $\tilde{\rho}^2(\mathbf{q})$ are Fourier transforms of the nucleon densities $\rho(\mathbf{r})$ and squared nuclear densities $\rho^2(\mathbf{r})$. Expanding the nucleon densities for axial-symmetric distributions in spherical harmonics we get

$$\rho(\mathbf{r}) = \sum_{\lambda} \rho_{\lambda}(r) Y_{\lambda 0}(\theta, 0) \quad (3.103)$$

Then

$$\tilde{\rho}(\mathbf{q}) = 4\pi \sum_{\lambda} i^{\lambda} Y_{\lambda 0}(\theta_q, 0) \int_0^{\infty} r^2 dr \rho_{\lambda}(r) j_{\lambda}(qr) \quad (3.104)$$

$$\begin{aligned} \tilde{\rho}^2(\mathbf{q}) &= \sqrt{4\pi} \sum_{\lambda} \frac{i^{\lambda}}{\tilde{\lambda}} Y_{\lambda 0}(\theta_q, 0) \sum_{\lambda' \lambda''} \hat{\lambda}' \hat{\lambda}'' (C_{00}^{\lambda \lambda' \lambda''})^2 \\ &\times \int_0^{\infty} r^2 dr \rho_{\lambda'}(r) \rho_{\lambda''}(r) j_{\lambda}(qr) \end{aligned} \quad (3.105)$$

Fourier transform of the effective $N - N$ interaction

The various components entering in the expression of the effective $N - N$ interaction have to be Fourier transformed in order to evaluate the oscillating integrals (3.64). When dealing with the M3Y forces the radial dependence is of the Yukawa type $\exp(-\nu r)/r$. Then the Fourier transform reads

$$\tilde{v}_Y(q) = \frac{4\pi}{q^2 + \nu^2} \quad (3.106)$$

For the delta kernel $\delta(r)$ the transform is

$$\tilde{v}_{\delta}(q) = 1 \quad (3.107)$$

3.3.4 The double-folding of the Coulomb interaction

The proton-proton Coulomb interaction is given by the well known formula

$$v_C(r) = \frac{e^2}{r} \quad (3.108)$$

where $e^2 = 1.4399 \text{ MeV fm}$ is the square of the unit charge. Then, neglecting the current distribution in the interaction he have the following double folding integral for the Coulomb potential

$$V_C(\mathbf{R}) = \int d\mathbf{r}_1 \int d\mathbf{r}_2 \frac{\rho_1(\mathbf{r}_1)\rho_2(\mathbf{r}_2)}{|\mathbf{R} + \mathbf{r}_2 - \mathbf{r}_1|} \quad (3.109)$$

In the most simple case, when we assume that both nuclei are spherical and the densities homogenous $\rho_i(R) = \rho_{oi}\Theta(R_i - R)$ [35]

$$V_C(R) = \frac{Z_1 Z_2 e^2}{R} \begin{cases} \frac{1}{2} \frac{R}{R_1} \left[3 - \frac{3}{5} \frac{R_2^2}{R_1^2} - \frac{R_2^2}{R_1^2} \right], & R \leq R_1 - R_2 \\ \left\{ 1 - \frac{3}{16} \frac{(R_1 + R_2 - R)^4}{R_1^2 R_2^2} \right. \\ \quad \times \left. \left[1 - \frac{2}{15} \frac{(R_1 + R_2 - R)(5R_1 + 5R_2 + R)}{4R_1 R_2} \right] \right\}, & R_1 - R_2 < R \leq R_1 + R_2 \\ 1, & R > R_1 + R_2 \end{cases} \quad (3.110)$$

In the case when both charge distribution are non-spherical the standard prescription is to expand $|\mathbf{R} + \mathbf{r}_2 - \mathbf{r}_1|$ into powers of either r_1 or r_2 by means of the formula [17]

$$\frac{1}{|\mathbf{R} + \mathbf{r}_2 - \mathbf{r}_1|} = \sum_{\lambda_1 \mu_1} \frac{4\pi}{2\lambda_1 + 1} \frac{r_1^{\lambda_1}}{|\mathbf{R} + \mathbf{r}_2|^{\lambda_1 + 1}} Y_{\lambda_1 \mu_1}(\omega_1) Y_{\lambda_1 \mu_1}^*(\Omega - \omega_2) \quad (3.111)$$

where we have assumed that $r_1 < |\mathbf{R} - \mathbf{r}_2|$. A similar expansion can be made in powers of r_1 under the condition $r_2 < |\mathbf{R} + \mathbf{r}_1|$. From these two expansions we may conclude

$$\frac{1}{|\mathbf{R} + \mathbf{r}_2 - \mathbf{r}_1|} = \sum_{\substack{\lambda_1 \lambda_2 \lambda_3 \\ \mu_1 \mu_2 \mu_3}} a(\lambda_1, \lambda_2, \lambda_3, \mu_1, \mu_2, \mu_3) \frac{r_1^{\lambda_1} r_2^{\lambda_2}}{R^{\lambda_3 + 1}} Y_{\lambda_1 \mu_1}(\omega_1) Y_{\lambda_2 \mu_2}(\omega_2) Y_{\lambda_3 \mu_3}(\Omega) \quad (3.112)$$

provided that $R > r_1 + r_2$. The dependence of the coefficients on the indices μ_1, μ_2 and μ_3 can be determined from the condition that the expression is a scalar under rotations of the coordinate system

$$a(\lambda_1, \lambda_2, \lambda_3, \mu_1, \mu_2, \mu_3) = \begin{pmatrix} \lambda_1 & \lambda_2 & \lambda_3 \\ \mu_1 & \mu_2 & \mu_3 \end{pmatrix} c(\lambda_1, \lambda_2, \lambda_3) \quad (3.113)$$

When the nuclear densities are not overlapping the terms with $\lambda_3 = \lambda_1 + \lambda_2$ are dominating. Consequently

$$c(\lambda_1, \lambda_2) = (4\pi)^{3/2} (-1)^{\lambda_2} \sqrt{\frac{(2\lambda_1 + 2\lambda_2)!}{(2\lambda_1 + 1)!(2\lambda_2 + 1)!}} \quad (3.114)$$

Then

$$\frac{1}{|\mathbf{R} + \mathbf{r}_2 - \mathbf{r}_1|} = \sum_{\substack{\lambda_1 \lambda_2 \\ \mu_1 \mu_2}} c(\lambda_1, \lambda_2) \begin{pmatrix} \lambda_1 & \lambda_2 & \lambda_1 + \lambda_2 \\ \mu_1 & \mu_2 & -\mu_1 - \mu_2 \end{pmatrix} \frac{r_1^{\lambda_1} r_2^{\lambda_2}}{R^{\lambda_1 + \lambda_2 + 1}} \\ \times Y_{\lambda_1 \mu_1}(\omega_1) Y_{\lambda_2 \mu_2}(\omega_2) Y_{\lambda_1 + \lambda_2, -(\mu_1 + \mu_2)}(\Omega) \quad (3.115)$$

Introducing the electric multipole tensors defined with respect to the space-fixed system (primed axes in Fig.3.4)

$$Q_{\lambda\mu} = \int \rho_p(\mathbf{r}) r^\lambda Y_{\lambda\mu}(\hat{\mathbf{r}}) \quad (3.116)$$

where ρ_p is the charge density distribution, the following analytical formula is obtained for the Coulomb interaction [36]

$$V_C(R) = \sum_{\substack{\lambda_1 \lambda_2 \\ \mu_1 \mu_2}} c(\lambda_1, \lambda_2) \begin{pmatrix} \lambda_1 & \lambda_2 & \lambda_1 + \lambda_2 \\ \mu_1 & \mu_2 & -\mu_1 - \mu_2 \end{pmatrix} \frac{1}{R^{\lambda_1 + \lambda_2 + 1}} \\ \times Q_{\lambda_1 \mu_1}^{(1)} Q_{\lambda_2 \mu_2}^{(2)} Y_{\lambda_1 + \lambda_2, -(\mu_1 + \mu_2)}(\Omega) \quad (3.117)$$

Transforming the electric multipole operators into the intrinsic coordinate (body-fixed) system (analogous to (3.56))

$$Q_{\lambda\mu}^{(i)} = \sum_{\mu'} D_{\mu\mu'}^\lambda(\omega_i) Q_{\lambda\mu'}^{(i)} \quad (3.118)$$

we arrive at the form bellow provided we consider only quadrupole and hexadecapole deformations [37]

$$V_C(R, \beta_1, \beta_2) = \frac{Z_1 Z_2 e^2}{R^2} \\ + \sqrt{\frac{4\pi}{5}} \frac{e}{R^3} \left[Z_1 P_2(\cos \beta_2) Q_{20}^{(2)} + Z_2 P_2(\cos \beta_1) Q_{20}^{(1)} \right] \\ + \frac{\sqrt{4\pi}}{3} \frac{e}{R^5} \left[Z_1 P_4(\cos \beta_2) Q_{40}^{(2)} + Z_2 P_4(\cos \beta_1) Q_{40}^{(1)} \right] \\ + 12\pi \sqrt{\frac{14}{5}} \frac{1}{R^5} Q_{20}^{(1)} Q_{20}^{(2)} \sum_{\mu=-2}^2 \begin{pmatrix} 2 & 2 & 4 \\ \mu & -\mu & 0 \end{pmatrix} d_{\mu 0}^2(\beta_1) d_{-\mu 0}^2(\beta_2) \quad (3.119)$$

If the fragments have ellipsoidal shape and sharp surfaces, the diffuseness is accounted only by the nuclear interaction as pointed out in [38], then the electric multipole moment of fragment 1 reads

$$Q_{\lambda 0}^{(1)} = \rho_{01} \int_0^{4\pi} d\Omega Y_{\lambda 1 0}(\Omega) \int_0^{R_1(\Omega)} dr r^{\lambda_1 + 2} \\ = 4\pi \rho_{01} \frac{\sqrt{2\lambda_1 + 1}}{\lambda_1 + 3} \int_{-1}^{+1} dx P_{\lambda_1}(x) [R_1(x)]^{\lambda_1 + 3} \quad (3.120)$$

where

$$R_1(x) = \frac{a_1}{\left[1 - \left(1 - \frac{a_1^2}{c_1^2}\right) x^2\right]} \quad (3.121)$$

is the equation in polar coordinates of the radius vector of spheroid 1. Using the following integral formula for the Legendre functions [39]

$$\int_{-1}^{+1} \frac{P_{2n}(x) dx}{(1 + kx^2)^{n+3/2}} = \frac{2(-k)^n}{(2n+1)(1+k)^{n+1/2}}, \quad (-1 < k < 1) \quad (3.122)$$

we obtain for λ even

$$Q'_{\lambda_0(1)} = 4\pi \frac{\sqrt{2\lambda_1 + 1}}{(\lambda_1 + 1)(\lambda_1 + 3)} 3Z_1 (c_1^2 - a_1^2)^{\lambda_1/2} \quad (3.123)$$

Introducing the definitions

$$x_{1,2}^2 = \frac{c_{1,2}^2 - a_{1,2}^2}{R^2} \quad (3.124)$$

the Coulomb interaction reads [40]

$$\begin{aligned} V_C(R, \beta_1, \beta_2) &= \frac{Z_1 Z_2 e^2}{R} \sum_{j=0}^{\infty} \sum_{k=0}^{\infty} \frac{3}{(2j+1)(2j+3)} \frac{3}{(2k+1)(2k+3)} \frac{(2j+2k)!}{(2j)!(2k)!} \\ &\times x_1^{2j} x_2^{2k} P_{2j}(\cos \beta_1) P_{2k}(\cos \beta_2) \end{aligned} \quad (3.125)$$

When the fragments symmetry axes are aligned, i.e. $\beta_1 = \beta_2 = 0$, Quentin showed that the above double series is converging for $|x_1| + |x_2| < 1$ and the final result is given, according to [41], in closed form :

$$\begin{aligned} V_C &= \frac{3Z_1 Z_2 e^2}{40R^2} \left\{ \frac{1}{x_1^2 x_2^2} (1 + 11x_1^2 + 11x_2^2) \right. \\ &+ P_{x_1} P_{x_2} \left[\frac{(1 + x_1 + x_2)^3}{x_1^3 x_2^3} \ln(1 + x_1 + x_2) \right. \\ &\left. \left. (1 - 3x_1 - 3x_2 + 12x_1 x_2 - 4x_1^2 - 4x_2^2) \right] \right\} \end{aligned} \quad (3.126)$$

3.4 Proximity Potential Model

One of the most simple macroscopic interaction between two deformable bodies whose surfaces have small curvature and diffuseness was formulated in the seventies on the basis of the "proximity force theorem" [42]. Before that it was Bass [43] who derived a proximity formul for two spherical nuclei. For that he considered two infinitely extended nuclear mater distributions with flat surfaces with a distance s between them. Then for the surface energy per elementary surface the following Ansatz was choosed

$$\frac{dE}{dS} = 2\gamma[1 - e(s)] \quad (3.127)$$

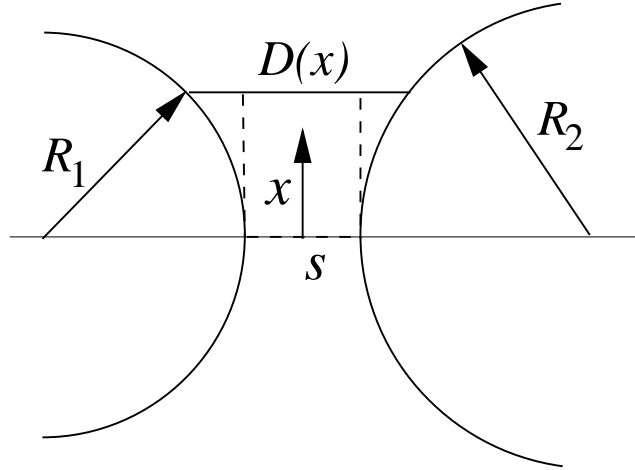


Figure 3.5: Two nuclei are treated in the proximity approximation as endless extended nuclear matter distributions. Due to the curved surface of realistic nuclei the distance D between two opposing points will increase with x . It is supposed that the radii R_i are large with respect to the minimal distance s the narrower laying surface points.

where

$$\gamma = 0.9517 \left[1 - 1.7826 \left(\frac{N - Z}{A} \right)^2 \right] \text{ MeV/fm}$$

is the surface energy coefficient and $e(s)$ is a function of the distance s , which takes into account the influence of the opposite matter distributions. Having these in mind the task is to compute the surface energy for two spherical nuclei with radii R_1 and R_2 .

The first hypothesis made is that the two radii are large compared to the distance s between the two surfaces. Then, the nuclear surfaces can be viewed approximately as endless extended nuclear matter distributions, with difference that now the surfaces are no longer flat but curved. The curvature determines that the distance D between two opposite points on the surfaces is no longer constant, but increase with x (see Fig.3.5).

Since the nuclei have spherical form, the dependence of D can be easily derived. For a sphere section we have the following relation

$$x^2 = 2RH - H^2 \quad (3.128)$$

where H is the thickness and x the halflength of the sphere's section. In the present approximation H is large compared to R , and therefore the quadratic term in the above formula can be neglected. We therefore obtain for the distance D as a function of x the following formula

$$D(x) = s + \frac{x^2}{2R_1} + \frac{x^2}{2R_2} \quad (3.129)$$

Integrating (3.127) over the surface we obtain

$$E_s = \gamma(S_1 + S_2) - 2\gamma \int dS e(D) \quad (3.130)$$

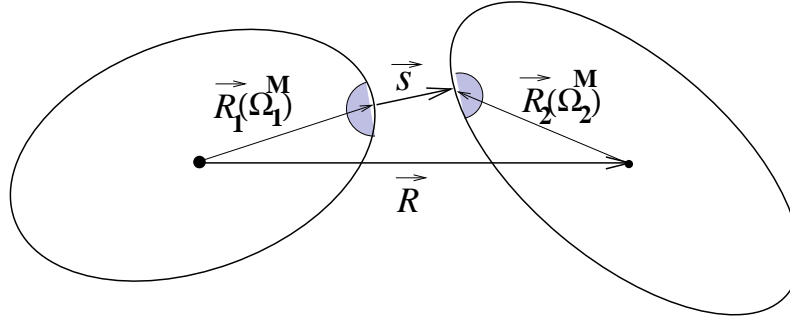


Figure 3.6: The minimal distance between the surfaces s is the shortest distance between the nuclear surfaces. The angles Ω_i^M are describing the closest laying points. They must be determined separately for each distance between the two centers, each deformation and each orientation.

The first term in the above formula represents the surface energy of both nuclei. The second one can be rewritten as

$$\gamma \int dS e(D) = 2\pi \int x dx e(D) = \pi \int d(x^2) e(D) \quad (3.131)$$

From (3.129) it follows easily that

$$dD = \frac{1}{2} \left(\frac{1}{R_1} + \frac{1}{R_2} \right) d(x^2) \quad (3.132)$$

and therefore

$$2\gamma \int dS e(D) = 4\pi\gamma \frac{R_1 R_2}{R_1 + R_2} \int_s^\infty dD e(D) \quad (3.133)$$

This integral $\int_s^\infty dD e(D)$ is the proximity function which is usually denoted by $\phi(x)$. The factor $\bar{R} = R_1 R_2 / (R_1 + R_2)$ is called the geometrical factor because it takes into account the nuclear form. The proximity formula was thus deduced for two spherical nuclei with half-density radii $R_{1,2}$ and the account only of terms of the order $s/R_{1,2}$.

The nuclear proximity potential is then defined as the difference between the total binding energy of the nucleus-nucleus system and the binding energies of the separated nuclei at infinity

$$V = -4\pi\gamma \bar{R} \phi(s) \quad (3.134)$$

Thus, the content of the proximity theorem is that the short-distance interaction energy can be written as the product of a function depending only on s and a factor, which takes into account the shape of the two nuclei [42].

The extension of theorem for a deformed target and spherical projectile was carried out in [44] and for two deformed nuclei in [45].

We present in what follows the formalism for two deformed nuclei according to [45].

In order to incorporate the orientation in the potential, a series of steps are fulfilled namely a) both nuclei are axial symmetric and thus the potential is independent of the Euler angle γ and b) the intrinsic axes $z'_{1,2}$ (see Fig.3.4) are laying in the same plane and therefore

also the dependence on the Euler angle is eliminated¹. In this case the interaction potential depends only on three coordinates $V(R, \beta_1, \beta_2)$. The minimal surface distance s is then determined by the angle Ω_i^M (see Fig.3.6)

$$s = \text{Min} |\mathbf{R} + \mathbf{R}_2(\Omega_2) - \mathbf{R}_1(\Omega_1)| = |\mathbf{R} + \mathbf{R}_2(\Omega_2^M) - \mathbf{R}_1(\Omega_1^M)| \quad (3.135)$$

This angle is in its turn determined by a numerical variational iterative procedure. The iteration must be carried out separately for any given set of coordinates.

Contrary to the spherical case the overlapping deformed nuclear forms cannot have only one s [46]. To overcome this problem the direction of s is taken parallel to the two-center distance \mathbf{R} . Here we deal with a conceptual problem. The interacting nuclear distributions are so densely localized that they can be described only by one coordinate. This is no longer the case at high densities.

According to Ref.[42] the geometrical factor for two elliptic coaxial paraboloids with tip distance s , radii of curvature P_i and ρ_i in the principal planes of curvature through the tip of paraboloid i , and an azimuthal angle φ between the principal planes of curvature

$$\bar{R} = \left\{ \frac{1}{P_1\rho_1} + \frac{1}{P_2\rho_2} + \left(\frac{1}{P_1P_2} + \frac{1}{\rho_1\rho_2} \right) \sin^2 \varphi + \left(\frac{1}{P_1\rho_2} + \frac{1}{P_2\rho_1} \right) \cos^2 \varphi \right\} \quad (3.136)$$

Due to the short-range of the nuclear potential only the dashed regions in Fig.3.6 are important and this is the justification for trading the deformed nuclei for two paraboloids. The radii of curvature must be taken at the surface points specified by the angles Ω_i^M and in the direction of their tangential plane. Due to the requirement that s is the minimum distance between the nuclear surfaces \mathbf{s}/s and $-\mathbf{s}/s$ are the normal vectors of the tangential plane of nuclei 1 and 2, respectively.

For axially symmetric nuclei the radius of curvature P is along the unit vector \mathbf{e}_θ and reads

$$P(\theta^M) = \frac{[R^2(\theta^M) + R'^2(\theta^M)]^{3/2}}{R^2 + 2R'^2 - 2RR''} \quad (3.137)$$

where $R' = \partial R/\partial \theta$. The radius of curvature is along \mathbf{e}_ϕ (see Fig.3.7). First we define ρ_\perp as the radius of curvature with the principal plane parallel to the intrinsic z -axis

$$\rho_\perp = R(\theta^M) \sin \theta^M \quad (3.138)$$

The theorem of Meusnier yields a connection between the radii of curvature through the same point but in relation to different planes

$$\rho_\perp = \rho \cos \gamma \quad (3.139)$$

where γ is the angle between the normal vector and ρ_\perp . The angle β between $R(\theta^M)$ and the normal vector is

$$\tan \beta = -\frac{1}{R} \frac{dR}{d\theta} = -\frac{R'}{R} \quad (3.140)$$

¹Note that this restriction has not been operated in the study of the orientation dependence of the double-folding potential

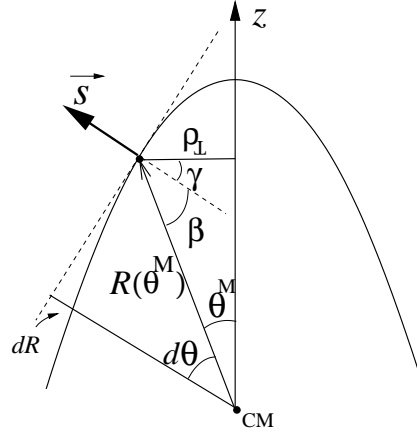


Figure 3.7: The display of the geometrical quantities necessary in the calculation of ρ

Besides, we infer from Fig.3.7 that

$$\gamma = \frac{\pi}{2} - \theta^M - \beta$$

The last four equations are finally providing

$$\rho(\theta^M) = \frac{R(\theta^M) \sin \theta^M}{\cos \left[\frac{\pi}{2} - \theta^M - \text{atan} \left(\frac{R'}{R} \right) \right]} \quad (3.141)$$

This equation is undetermined at the tip of the nucleus ($\theta^M=0$). However due to the axial symmetry we have at this point

$$P(\theta^M) = \rho(\theta^M) \quad (3.142)$$

As shown in ref.[47] \bar{R} , which depends on the rate of curvature κ of both interacting nuclei, can be put in the form

$$\bar{R} = \frac{1}{\sqrt{(\kappa_1^{\parallel} + \kappa_2^{\parallel})(\kappa_1^{\perp} + \kappa_2^{\perp})}} \quad (3.143)$$

where

$$\kappa_i^{\parallel} = \frac{R_i^2 + R_i^3 \left(\frac{\partial^2}{\partial \phi^2} \frac{1}{R_i} \right)}{\left[R_i^2 + \left(\frac{\partial R_i}{\partial \phi} \right)^2 \right]^{3/2}} \quad (3.144)$$

and

$$\kappa_i^{\perp} = \frac{R_i^2 + R_i^3 \left(\frac{\partial^2}{\partial \theta^2} \frac{1}{R_i} \right)}{\left[R_i^2 + \left(\frac{\partial R_i}{\partial \theta} \right)^2 \right]^{3/2}} \quad (3.145)$$

and the argument of the proximity function will also depend on orientation angles

$$s = r - R_1^{(0)} \left(1 + \sum_{\lambda\mu} \alpha_{\lambda\mu}^{(1)} Y_{\lambda\mu}^*(\theta, \phi - \phi_1) \right) - R_2^{(0)} \left(1 + \sum_{\lambda\mu} \alpha_{\lambda\mu}^{(2)} Y_{\lambda\mu}^*(\pi - \theta, \pi + \phi - \phi_2) \right) \quad (3.146)$$

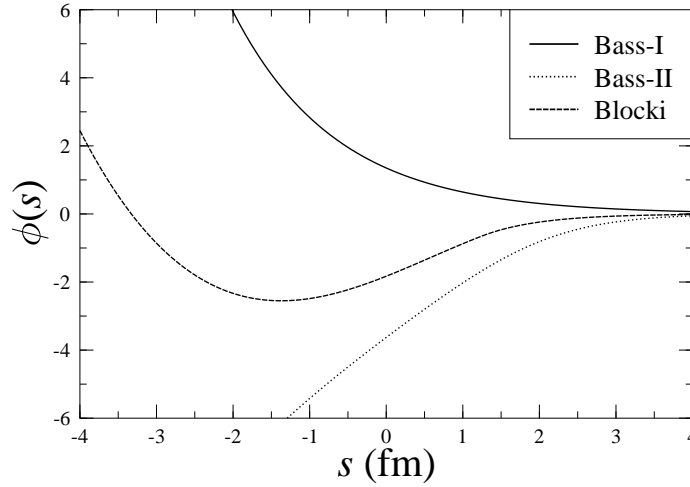


Figure 3.8: Comparison of different proximity functions. The proximity function of Blocki et al. (dashed line) increases when the nuclei are overlapping.

The next step consists in the determination of the proximity function $\phi(s)$. Bass used as an empirical law an exponential function [43],

$$\phi(s) = \frac{d}{1[\text{fm}]} e^{-\frac{s}{d}}, \quad (3.147)$$

where $d=1.35$ fm, which later [48], upon better agreement with fusion data was modified to

$$\phi(s) = \{4\pi\gamma(A \exp(s/d_1) + B \exp(s/d_2))\}^{-1} \quad (3.148)$$

where $A=0.0300$ MeV⁻¹fm, $B = 0.0061$ MeV⁻¹fm, and $d_1=3.30$ fm and $d_2=0.65$ fm, these last two constants determining the range of the interaction.

Blocki et al. [42] used the Seyler-Blanchard effective $N - N$ interaction and the Thomas-Fermi model and integrated numerically over the surface using a Fermi-density profile

$$\rho(\mathbf{r}) = \frac{\rho_0}{1 + \exp[(r - R(\Omega))/0.872]}$$

The result was

$$\begin{aligned} \phi(s \leq 1.2511\text{fm}) &= -\frac{1}{2}(s - s_0)^2 - 0.0852(s - s_0)^3 \\ \phi(s \geq 1.2511\text{fm}) &= -3.437 \exp(-s/0.75\text{fm}) \end{aligned} \quad (3.149)$$

where $s_0=2.54$ fm. In Fig. 3.8 we compare $\phi(s)$ for the two Bass ansatz, (3.147, 3.148) and the Blocki one (3.149). It is noticeable the increase of the (3.149) ansatz for negative s , which corresponds to a compression energy as discussed in the preceding section. The second ansatz of Bass (3.148) has also this tendency but instead it is purely repulsive. The repulsive behaviour of the proximity function (3.149) is caused by the nucleon relative impulse dependent term in the Seyler-Blanchard interaction

$$v(r_{12}, p_{12}) = -328.61 \frac{e^{-r_{12}/a}}{r_{12}/a} \left(1 - \frac{p_{12}}{b^2}\right) \quad (3.150)$$

with $a=0.62567$ fm and $b=392.48$ MeV/ c

3.5 Self-consistent methods

3.5.1 The Hartree-Fock+BCS

The LDM, which is based on a semiclassical description of the nuclei, supplemented by the shell-effect corrective energy, is only a poor substitute for a self-consistent calculation [50]. One of the main advantages of the self-consistent HF+BCS calculation is that it provides simultaneously both the single-particle and semiclassical properties of nuclei. The general properties of the Hartree-Fock method were reviewed in [51, 52]. In what follows we will sketch briefly the underlying ideas of this method.

According to the variational principle, the ground-state of an A -body system is that completely antisymmetric state $\Psi(1, \dots, A)$ which minimizes the expectation value of the corresponding Hamiltonian $\langle \Psi | H | \Psi \rangle$ subject to the condition that $\langle \Psi | \Psi \rangle = 1$. This can be included in the variational problem by introducing the Lagrange multiplier E , and demanding a minimum of

$$\langle \Psi | H | \Psi \rangle - E(\langle \Psi | \Psi \rangle - 1) \quad (3.151)$$

This implies

$$\langle \delta \Psi | H | \Psi \rangle = 0, \quad (3.152)$$

for all variations of $|\delta \Psi\rangle$, together with

$$\delta E(\langle \Psi | \Psi \rangle - 1) = 0 \quad (3.153)$$

for arbitrary variations δE . Since $|\delta \Psi\rangle$ is arbitrary, the variational principle leads to the Schrödinger equation

$$(H - E) | \Psi \rangle = 0 \quad (3.154)$$

The variational method consists in introducing a trial wave function $f(q_1, q_2, \dots)$ depending on a certain number of parameters $(q_1, q_2, \dots) \equiv \mathbf{q}$. These parameters are varied until

$$\langle \Psi | H | \Psi \rangle - (\langle \Psi | \Psi \rangle - 1) = \mathcal{H}(\mathbf{q}) - E(N(\mathbf{q}) - 1) \quad (3.155)$$

reaches a minimum. Necessary conditions for a stationary value are

$$\frac{\partial \mathcal{H}}{\partial q_i} - E \frac{\partial N}{\partial q_i} = 0; \quad N(\mathbf{q}) = 1 \quad (3.156)$$

The Hartree-Fock approximation is an application of the variational method, which utilizes a large number of variational parameters. Hartree's idea was to ascribe to each particle a state, or single particle orbital $\phi_i(r_i)$, so that the total wave-function Ψ is a product of these orbitals. Fock introduced antisymmetry by making a Slater determinant rather than a simple product

$$\Psi(1, \dots, A) = \frac{1}{\sqrt{A!}} \det[\phi_i(r_j)] = \frac{1}{\sqrt{A!}} \sum_P (-1)^P \phi_1(r_{j_1}) \dots \phi_1(r_{j_A}) \quad (3.157)$$

Table 3.2: Parameters of the Skyrme interactions SII and to SVI

Interaction	t_0 (MeV·fm ³)	t_1 (MeV·fm ⁵)	t_2 (MeV·fm ⁵)	t_3 (MeV·fm ⁶)	x_0	W (MeV·fm ⁵)
SII	-1169.9	586.6	-27.1	9331.1	0.34	105.0
SIII	-1128.75	395.0	-95.0	14000.0	0.45	120.0
SIV	-1205.6	765.0	35.0	5000.0	0.05	150.0
SV	-1248.29	970.56	107.22	0.0	-0.17	150.0
SVI	-1101.81	271.67	-138.33	17000.0	0.583	115.0

In the above formula the symbols $(j_1 \dots j_A)$ are a permutation P of the labels $1, \dots, A$ and $(-1)^P$ is the signature of the permutation. To ensure that the wave-function $|\Psi\rangle$ is normalized, the orbitals $\phi_i(r)$ form an orthonormal set.

Brink and Vautherin were the first to carry out HF calculations reviving a very simple form of effective interaction, originally suggested by Skyrme, which contains only a small number of adjustable parameters [53]. It is of the form $V_2 + V_3$ where

$$\begin{aligned}
V_2 = & t_0(1 + x_0 P_\sigma)\delta(r_{12}) + \frac{t_1}{2}(1 + x_1 P_\sigma)(k'\delta(r_{12}) + \delta(r_{12})k^2) \\
& + t_2(1 + x_2 P_\sigma)\delta(r_{12})\mathbf{k}' \cdot \delta(r_{12})\mathbf{k} + iW(\boldsymbol{\sigma}^1 + \boldsymbol{\sigma}^2) \cdot (\mathbf{k}' \times \delta(r_{12})\mathbf{k}) \quad (3.158)
\end{aligned}$$

where P_σ is the spin exchange operator, \mathbf{k} is the operator $(-i\nabla)$ acting to right and \mathbf{k}' to left. V_3 incorporates a suitable density dependence. Originally it was taken to be a contact three-body force

$$V_3 = t_3\delta(r_{12})\delta(r_{23}) \quad (3.159)$$

but subsequently it has been found preferable to consider it a density dependent two-body force

$$V'_2 = \frac{t_3}{6}(1 + x_3 P_\sigma)\rho_0^\alpha\delta(r_{12}) \quad (3.160)$$

(for $x_3 = 1$, $\alpha = 1$, this force makes the same contribution to the Hartree-Fock energy as does V_3).

There are several sets of Skyrme force parameters which have been fitted to reproduce nuclear properties over a wide region of the the Periodic Table. These have names S-I, S-II, etc. and are listed in table 3.2 for 5 choices. In most cases the exchange parameters are set to zero, $x_3 = 1$ and $\alpha = 1$. This leaves six real parameters t_0, x_0, t_1, t_2, t_3 and W , the strength of the spin-orbit interaction. A value of $W = 120\text{MeV}\cdot\text{fm}^5$ gives reasonable spin-orbit splittings for the eigenvalues near magic nuclei. The various Skyrme forces can be characterized by the value of t_3 , the amount of density dependence.

The Skyrme forces not only reproduce a large amount of nuclear data from a small number of adjustable parameters and they are exceedingly easy to use. The zero range nature of

the force ensures that the Hartree-Fock fields are local, and in fact are simple polynomials of local densities.

In our study for the HF part of the interaction we choosed the Skyrme interaction SIII [54], which succeeded to reproduce satisfactory the single-particle spectra of even-even nuclei. The difference between the binding energy computed with SIII and the experimental one appears to be, for a large number of nuclei, ≈ 5 MeV [55]. It also produces a fairly well $N - Z$ dependence of the binding energy[56]. The present work considers nuclei that are not in a closed shell configuration. Thus, the level occupations will have a large effect on the solution of the HF equations.

Usually the HF method is extended to the Hartree-Fock Bogolyubov (HFB) formalism by using a mixture of different configurations in place of a single Slater determinant. However, when dealing with a Skyrme force which has been simplified such that the bulk properties of the nucleus are reproduced, one would have to introduce additional parameters in order to guarantee that sensible pairing matrix elements are obtained.

Following Vautherin [57] we assign to each orbital ϕ_k an occupation number $n_k = v_k^2$, where $u_k^2 + v_k^2 = 1$, $u_{\bar{k}} = u_k$ and $v_{\bar{k}} = -v_k$. In terms of the density $\rho(\mathbf{r}) = 2 \sum'_k n_k |\phi_k(\mathbf{r})|^2$ the HF+BCS total energy, that has to be minimized, reads

$$E_{\text{HF+BCS}} = \text{Tr} \left[\left(T + \frac{1}{2} \mathcal{V} \right) \rho \right] + E_p \quad (3.161)$$

where

$$\langle T \rangle = \frac{\hbar^2}{m} \left(1 - \frac{1}{A} \right) \sum'_k n_k \int d\mathbf{r} |\phi_k(\mathbf{r})|^2 \quad (3.162)$$

is the expectation value of the kinetic energy, $\mathcal{V} = \text{Tr}(\rho \tilde{v})$ enters as the Hartree-Fock-like potential, \tilde{v} being the antisymmetrized effective two-body interaction. The primed sum \sum' denotes a sum over all HF orbitals having projections of the total angular momentum \mathbf{j} on the z -axis $\Omega_k > 0$. To the total energy we added the pairing energy

$$E_p = -\frac{G}{4} \left\{ \sum_k \left[n_k (1 - n_k)^{\frac{1}{2}} \right] \right\}^2 \quad (3.163)$$

For BCS-like calculations, the matrix elements of \tilde{v} between HF states is taken to be constant

$$G = - \int d\mathbf{r} \int d\mathbf{r}' \phi_k^*(\mathbf{r}) \phi_{\bar{k}}^*(\mathbf{r}) \tilde{v}(\mathbf{r}, \mathbf{r}') \phi_l(\mathbf{r}) \phi_{\bar{l}}(\mathbf{r}) \quad (3.164)$$

Varying the normalized single-particle wave functions ϕ_k and their amplitudes v_k under the additional constraint $\lambda_\tau \sum_k (\delta_{\tau k, \tau} n_k - N_\tau)$, ($\tau = p, n$), which ensures that on the average the system contains the correct number of neutrons N and protons Z , we are lead to the standard HF and BCS equations [57].

The occupations n_k are determined at each step of the HF iterative calculation using the HF eigenvalues ε_k , and they are employed at the next step to construct the HF field. The pairing force constant is

$$G_\tau = \frac{G_{0\tau}}{11 + N_\tau} \text{ MeV} \quad (\tau = p, n) \quad (3.165)$$

The constant $G_{0\tau}$ was adjusted in such a way to obtain the experimental pairing gap

$$\Delta_\tau = G \sum_k' u_k v_k \quad (3.166)$$

In the deformed HF calculations one have to optimize the basis which is choosen to correspond to an axial symmetric deformed harmonic-oscillator with frequencies ω_\perp and ω_z . Such a basis is characterized by the deformation parameter $q = \omega_\perp/\omega_z$ and harmonic oscillator length $b = \sqrt{m\omega_0/\hbar}$, with $\omega_0^3 = \omega_\perp^2\omega_z$. The basis is cut off after N_{max} major shells, where $N_{max}=10$ or 12 for the nuclei emerging in the sf of ^{252}Cf [58].

The next step consists in mapping out the potential energy curves by constraining our HF+BCS calculations in which a quadratic constraint $\frac{C}{2}(Q - Q_0)^2$ is added to the energy functional (3.161) [59]. Here Q_0 is a specified targed value of the mass quadrupole moment.

Bibliography

- [1] D.J.Thouless, *The Quantum Mechanics of Many-Body Systems*, Academic Press, New York (1961).
- [2] C.F. von Weizsäcker, *Die Atomkerne - Grundlagen und Anwendungen Ihrer Theorie*, Akademische Verlagsgesellschaft M.B.H, Leipzig 1937.
- [3] W.D.Myers and W.J.Swiatecki, Nucl.Phys.**A81** (1966) 1.
- [4] V. V. Pashkevich, Nucl.Phys.**A169** (1971) 275
- [5] H.J.Krappe and J.R.Nix, in *Proceedings of the Third international Atomic Energy Agency Symposium on the Physics and Chemistry of Fission, Rochester, New York, 1973* (International Atomic Energy Agency, Vienna, 1974), Vol.I, p.159.
- [6] H.J.Krappe, J.R.Nix and A.J.Sierk, Phys.Rev.**C20**, (1979) 992.
- [7] K.T.R.Davies and J.R.Nix, Phys.Rev.**C14**, (1976) 1977.
- [8] R. W. Hasse and W. D. Myers *Geometrical Relationships of Macroscopic Nuclear Physics Equations*, (Springer Verlag, Berlin, 1988)
- [9] H.Schultheis and R.Schultheis, Nucl.Phys.**A215** (1973) 329.
- [10] G.R.Satchler and W.G.Love, Phys.Rep.**55** (1979) 183.
- [11] M.E.Brandan and G.R.Satchler, Phys.Rep.**285** (1997) 143.
- [12] H.Feshbach, *Theoretical Nuclear Physics*, Vol.II (John Wiles & Sons, New York, 1992)
- [13] Ş. Mişicu and W.Greiner, Phys.Rev.**C66**, 044606 (2002).
- [14] G.R.Satchler, *Direct Nuclear Reactions*, Clarendon Press, Oxford, 1983.
- [15] F. Carstoiu and R.J. Lombard, Ann. Phys. (N.Y.) **217**, 279 (1992).
- [16] P. Möller, J.R. Nix, W.D. Myers, and W.J. Swyatecki, At. Data Nucl. Data Tables **59**, 185 (1995).
- [17] D.A.Varshalovich, A.N.Moskalev and V.K.Hersonskii, *Kvantovaya Teoriya Uglovogo Momenta*, Izdatelstvo Nauka, Leningrad 1975.

-
- [18] W.G.Love and L.W.Owen, Nucl.Phys.**A239** (1975) 74.
- [19] G.Bertsch, W.Borysowicz, H. McManus and W.G.Love, Nucl.Phys.**A284** (1977) 399.
- [20] W.G.Love and L.W.owen, Nucl.Phys.**A239** (1975) 74.
- [21] D.T.Khoa, W.von Oertzen and H.G.Bohlen, Phys.Rev.**C49** (1994) 1652.
- [22] D.T.Khoa and W.von Oertzen, Phys.Lett.**B342** (1995) 6.
- [23] A.M.Kobos, B.A.Brown, R.Lindsay and G.R.Satchler, Nucl.Phys.**A384** (1982) 65.
- [24] J.P.Jeukene, A.Lejeune and C.Mahaux, Phys.Rev.**C16** (1977) 80.
- [25] H.A.Bethe, Ann.Rev.Nucl.Sci.**21** (1971) 92.
- [26] Y.Schutz *et al.*, Nucl.Phys.**A599**, 97c (1996).
- [27] J.P.Blaizot, J.F.Berger, J.Dechargé and M.Girod, Nucl.Phys.**A591**, 435 (1995).
- [28] K.Wildermuth and E.J.Kanelopoulos, Reports on Progress in Physics**42**, 1719 (1979).
- [29] P.Holzer, U.Mosel and W.Greiner, Nucl.Phys.**A138**, 241 (1969).
- [30] E.Uegaki and Y.Abe, Progr.Theor.Phys., **90** (1993) 615.
- [31] W.D.Myers and W.J.Swiatecki, Phys.Rev.**C57**, 3020 (1998)
- [32] Ş. Mişicu and D.Protopopescu, Acta Phys.Pol.**B30**, 127 (1999).
- [33] A.B.Migdal, *Theory of Finite Fermi Systems and Applications to Atomic Nuclei*, Nauka, Moscow 1982.
- [34] A.Săndulescu, F.Cârstoiu, Ş.Mişicu, A.Florescu, A.V.Ramayya, J.H.Hamilton and W.Greiner, J.Phys.G:Part.Nucl.**24**, 181-204 (1998).
- [35] H.Iwe and H.J.Wiebicke, preprint Rosendorf Zfk-297, Dubna 1978, JINR-E4-11967.
- [36] K.Adler and A.Winther, *Electromagnetic Excitation. Theory of Coulomb Excitation with Heavy Ions*, North-Holland Pub-Comp., Amsterdam 1975.
- [37] M.J. Rhoades-Brown, V.E.Oberacker and W.Greiner, Z.Phys.A-At.& Nucl.**310**, (1983) 287
- [38] W.Scheid and W.Greiner, Zeit.Phys.**130**, 159 (1951).
- [39] E.W.Hobson, *The Theory of Spherical and Ellipsoidal Harmonics*, Cambridge University Press, London, 1931, p.48, example 1.
- [40] J.R.Nix, *Studies in the Liquid-Drop Theory of Nuclear Fission*, report UCRL-11338, University of California, 1 April 1964.

- [41] P.Quentin, J.Phys.**30** (1969) 497.
- [42] J.Blocki, J.Randrup, W.J.Swiatecki and C.F.Tsang, Ann.Phys.N.Y.**105**, 427 (1977)
- [43] R.Baas, Nucl.Phys.A**231**, 45 (1974).
- [44] A.J.Baltz and B.F.Bayman, Phys.Rev.**C26** 1969 (1982)
- [45] M.Seiwert, W.Greiner, V.Oberacker and M.J.Rhoades-Brown, Phys.Rev.**C29** 477 (1984).
- [46] M.Seiwert, *Untersuchung des Kernpotentials in der Massregion überkritischer Systeme mittels phänomenologischer Modelle*, Disertation, J W Goethe Universität, Frankfurt am Main 1985.
- [47] R.A.BrogliA, C.H.Dasso and A.Winther, in Proceedings of the International School of Physics "Enrico Fermi", Course LXXVII : *Nuclear Structure and Heavy-Ion Collisions*, eds. R.A.BrogliA and R.A.Ricci, North-Holland Pub.Co, 1981.
- [48] R.Bass, Phys.Rev.Lett.**39** 265 (1977).
- [49] D.L.Hill and J.A.Wheeler, Phys.Rev.**89**, 1102 (1953).
- [50] M.Brack, J.Damgaard, A.S.Jensen, H.C.Pauli, V.M.Strutinsky and C.Y. Wong, Rev.Mod.Phys. **44** (1972) 320.
- [51] P. Quentin and H. Flocard, Ann.Rev.Nucl.Part.Sci.**28** (1978) 523.
- [52] P. Ring and P. Schuck, *The Nuclear Many-Body Problem*, Springer, New York 1980.
- [53] D.Vautherin and D.M.Brink, Phys.Rev.**C5** (1972) 626
- [54] M. Beiner, H. Flocard, Nguyen van Giai and P. Quentin, Nucl.Phys. A **238** (1975) 29.
- [55] P. Quentin, Thèse d'État, Université de Paris-Sud, France (1975).
- [56] N. Tajima, P.Bonche, H.Flocard, P.-H. Heenen and M.S. Weiss, Nucl.Phys. A **551** (1993) 434.
- [57] D.Vautherin, Phys.Rev. C **7** (1973) 296.
- [58] H.Flocard, P. Quentin and D.Vautherin, Phys.Lett. B **46** (1973) 304.
- [59] H.Flocard, P. Quentin, A.K.Kerman and D.Vautherin, Nucl.Phys. A **203** (1973) 433.